Aus dem Comprehensive Pneumology Center (CPC)
Vorstand: Prof. Dr. Erika von Mutius

Molecular and clinical characterization of malignant pleural effusions.

Dissertation

zum Erwerb des Doktorgrades der Medizin

an der Medizinischen Fakultät der

Ludwig-Maximilians-Universität zu München

vorgelegt von

Caroline Maria Hackl

aus

München

Jahr

2022

Mit Genehmigung der Medizinischen Fakultät der

Universität München

Berichterstatter:	Prof. Dr. Jürgen Behr
Mitberichterstatter:	Prof. Dr. Dennis Nowak Prof. Dr. Dominik Rüttinger
Mitbetreuung durch den promovierten Mitarbeiter:	Prof. Dr. Georgios Stathopoulos
Dekan:	Prof. Dr. med. Thomas Gudermann
Tag der mündlichen Prüfung:	14.07.2022

Contents

Summary

Malignant pleural effusions (MPE) affect an increasing portion of cancer patients worldwide and pose a major challenge for clinical cancer care. The diagnostic strategy to identify the underlying primary tumor is burdensome and treatment remains palliative. This thesis presents innovative approaches that might complement and optimize MPE diagnosis and therapy. Basic clinical data was used to develop a distinctive scoring system for effusion's etiology, the Mesothelioma Score. It is based on the criteria airway resistance, partial arterial pressure of oxygen at ambient air and hemoglobin. The score predicts mesothelioma with a sensitivity of 81.82% and a specificity of 95.24% and thus can be used as an introductory screening tool for patients presenting with MPE of unknown origin. Further, the recently proposed potential of pleural effusion as a liquid biopsy specimen was verified by determination of the *KRAS* and *EGFR* mutation status in paired cell pellets and supernatants of 40 MPE samples. Both oncogenes are believed to play a pathogenetic role in MPE induction. Activating mutations in the *KRAS* proto-oncogene (codon 12/13 and codon 61) were detected in 42.50% of cases, hence more frequently than stated in present studies. This might be explained by the extremely sensitive LOD of employed droplet digital PCR technique and is consistent with recent pathophysiologic insights in MPE's genotype-phenotype link. Besides, a substantial proportion of *KRAS* mutations was found in codon 61, a spot rarely sequenced though capable of MPE induction. *EGFR* exon 19 deletion mutations were detected in 12.50% of MPE samples and for 16.67% of patients with non-small-cell lung carcinoma. *KRAS* and *EGFR* mutations are both addressable by novel biologicals that have already proven their potential in halting MPE formation. Hence, pleural effusions can be used as repeatable diagnostic source for the longitudinal surveillance of a pleural tumors' genetic profile, thus guiding mutation-based targeted MPE treatment.

Zusammenfassung

Maligne Pleuraergüsse betreffen einen zunehmenden Anteil onkologischer Patienten weltweit und stellen eine wesentliche Herausforderung für die klinische Versorgung der Tumorpatienten dar. Die Differentialdiagnostik zugrundeliegender Tumorerkrankung ist beschwerlich und das therapeutische Vorgehen verbleibt palliativ. Diese Arbeit stellt innovative Ansätze vor, welche Diagnostik und Therapie maligner Pleuraergüsse ergänzen und optimieren könnten. Allgemeine klinische Daten wurden herangezogen, um ein Diagnosewerkzeug für die Ergussätiologie zu entwickeln. Der Mesotheliom Score basiert auf den Kriterien Atemwegswiderstand, arterieller Sauerstoffpartialdruck (bei Raumluft) und Hämoglobin. Der Score prognostiziert einen Primärtumor der Pleura mit einer Sensitivität von 81.82% und einer Spezifität von 95.24% und kann somit als Screening-Methode für Ergusspatienten mit unklarem Primarius genutzt werden. Indem der Mutationsstatus der Onkogene *KRAS* und *EGFR* in gepaarten Zell- und Überstandsproben 40 maligner Pleuraergüssen ermittelt wurde, konnte zudem der Nutzen des Ergussmaterials als alternative Gewebeprobe bestätigt werden. Beiden Onkogenen wird eine kausale Rolle in der Ergussentwicklung zugeschrieben. Aktivierende Mutationen im *KRAS* Proto-Onkogen (Kodon 12/13 und Kodon 61) wurden in 42.50% der Fälle und damit häufiger als in bestehenden Studien festgestellt. Dies kann in der sensitiven Nachweisgrenze der Droplet digital PCR Methode erklärt sein und steht im Einklang mit den jüngsten pathophysiologischen Erkenntnissen zur Ergusskompetenz eines Tumors. *EGFR* Mutationen in Exon 19 konnten in 12.50% der Ergussproben festgestellt werden, ebenso für 16.67% der Patienten mit nicht-kleinzelligem Lungenkarzinom. *KRAS* und *EGFR* Mutationen sind therapeutisch mittels neuartiger Biologika adressierbar, welche sich bereits als wirksam für das Ergussmanagement erwiesen haben. Pleuraergüsse können folglich wiederholt als diagnostisches Material zur Überwachung des genetischen Profils eines pleuralen Tumors genutzt werden und somit eine zielgerichtete, mutationsbasierte Therapie maligner Pleuraergüsse begründen.

List of figures

List of tables

List of abbreviations

CCL2	Chemokine ligand 2
cDNA	Cellular DNA
cfDNA	Circulating cell-free DNA
Ch	Channel
CP	Cell pellet
CRP	C-reactive protein
ddPCR	Droplet digital polymerase chain reaction
DL_{CO}	Diffusion capacity of the lung for carbon monoxide
EGFR	Epidermal growth factor receptor
EGFR ex19del	*EGFR* exon 19 deletion mutation
FAM	Carboxyfluorescein
FEV_1	Forced expiratory volume in one sec
FVC	Forced vital capacity
Hb	Hemoglobin
HEX	Hexachlorofluorescein
Hct	Hematocrit
$lymphocytes_{rel}$	Relative lymphocyte count
KRAS	Kirsten rat sarcoma viral oncogene homologue
LOD	Limit of detection
MEF_{50}	Mean expiratory flow at 50% of forced vital capacity
MEF_{75}	Mean expiratory flow at 75% of forced vital capacity
$MEF_{75/25}$	Mean expiratory flow between 75% and 25% of forced vital capacity
MPE	Malignant pleural effusion
n	Number
NSCLC	Non-small-cell lung carcinoma
otherCA	Other metastatic cancer
P	Probability
p_aO_2	Arterial partial pressure of oxygen
PEF	Peak expiratory flow
$protein_{tot}$	Total plasma protein
sR	Specific airway resistance
R	Airway resistance
RBC	Red blood cell count
ROC	Receiver operating characteristic
S_aO_2	Arterial oxygen saturation
SUP	Supernatant
TKI	Tyrosine kinase inhibitor

1 Introduction

1.1 Malignant pleural effusion - a challenging diagnosis

Malignant pleural effusion (MPE) is defined as fluid accumulation in the pleural space due to a primary or metastatic malignancy of the pleura. The diagnosis is based on cytological and/or histological criteria, precisely malignant cells in the pleural exsudate and/or malignant pleural invasion (1). MPE is a syndrome that affects up to 15% of all cancer patients (2). The majority of cases evolve with metastatic pleural carcinomatosis, most commonly due to non-small-cell lung carcinoma (NSCLC), in particular lung adenocarcinoma. Together with breast cancer, it accounts for up to 65% of all MPE cases (3). Mesothelioma, the most common primary pleural malignancy, comes along with pleural effusion in more than 90% of cases. With the increase in global cancer rate, MPE´s incidence is rising just like the associated healthcare costs (4). Prognosis remains palliative, with an overall survival between three and twelve months (5). It crucially depends on the causative cancer type (6) and time till treatment. In approximately 70% of cases, MPE occurs as the first symptome of an advanced malignancy (7). Accordingly, efficient differential diagnostics of MPE´s tumor of origin is vital for the appropiate treatment strategy and thus patients outcome. Current guidelines recommend fluid accquisition by pleurocentesis as the first diagnostic action. The diagnostic sensitivity of subsequent immunocytological analysis depends on cancer histology, sample quality and the expertise of the pathologist (8). Notably, the mean diagnostic yield of 60% is expected to be as low as 20% for mesothelioma (9). A reliable diagnosis frequently requires thoracoscopic biopsy. Not only does histologic examination increase the diagnostic sensitivity up to 90%, pleural biopsy also provides material for immunohistochemistry and genotyping (10). Still, distinguishing whether MPE is caused by a primary or metastatic pleural malignancy is challenging, as mesothelioma represents a brought range of cytomorphological and immunohistochemical features (11). Particularly, the differential diagnostics of epitheloid mesothelioma and adenocarcinoma tends to be inconclusive (12). The diagnostic sensitivity of cytohistologic modalities depicting mesothelioma ranges precariously between 32-76% (13). This becomes an even greater challenge when pleural effusion is the only available diagnostic source due to an inoperable tumor stage or poor overall performance status.

1.2 Novel pathophysiologic insights in MPE competence

Besides diagnostic restrictions, physicians have only limited treatment options. The majority of patients develop life quality restricting symptoms, above all debilitating breathlessness and cachexia (14). The treatment strategy remains palliative, aiming for symptomatic relief and life quality adjusted survival (2). Pleurodesis and pleurectomy yield radiologic improvement in the longer term, but along with prolonged and repeated hospitalization and the risk of significant complications, such as postoperative respiratory failure and post-VATS-chest wall pain (15,16). Hence minimal-invasive indwelling pleural catheters are commonly favored, as they enable outpatient symptomatic relief (17). Insights in MPE's genotype-phenotype link raise hope for forthcoming molecular targeted therapy (18–20). According to the current knowledge, pleural fluid accumulation is promoted by the proinflammatory, angiogenic and vasoactive potential of pleural-homed tumor cells (4). Approximately 60% of patients with pleural metastases develop MPE, but the reason for this dichotomous phenotype remains unknown (8). Concomitant sampling of a primary tumor and its pleural metastatic site (via pleural biopsy and/or MPE collection) revealed mutational discordance, indicative of clonal tumor cell evolution featuring MPE competence. Epidermal growth factor receptor (*EGFR*) mutations are enriched in pleural metastases and MPE compared to the primary tumor, hinting at the activated oncogene as a driver of metastatic pleural invasion and MPE formation (21). Resent in vivo studies have further determined mutant Kirsten rat sarcoma viral oncogene homologue (*KRAS*), a downstream factor of the *EGFR* pathway, as a molecular culprit of wet carcinomatosis. In mouse models, tumorigenic cell lines harboring *KRAS* mutations (in codon 12, 13 and 61) not only produced extensive pleural carcinomatosis but demonstrated MPE competence in contrast to *KRAS* wildtype cells lines. Mutant *KRAS* empowers the MPE-phenotype via paracrine, chemokine ligand 2 (CCL2)-dependent recruitment of myeloid cells to the pleural space, thus initiating and maintaining an inflammatory and vasoactive response that provokes pleural fluid accumulation. Biologic agents that prevent *KRAS* membrane transport (deltarasin, a phosphodiesterase PDEδ-KRAS interaction inhibitor) or interfere tumor-host-signaling (anti-CCL2-antibodies) appear effective in halting MPE formation. Mouse models demonstrate decreased MPE incidence, reduced volume and limited progression (18,22).

1.3 The advantages of liquid biopsies

Targeted cancer therapies are based on a tumor's individual genetic profile. Tissue biopsy is the current gold standard method for genomic analysis (23), but with some limitations. Tissue-based molecular analysis is subject to sampling bias as it provides only a glimpse in a tumors' temporal and spatial heterogeneity. Tumor evolution results in dynamic intratumor multiclonality and phenotypic plasticity (24,25). Hence, MPE should rather be considered a distinct cancer phenotype than merely a complication of malignancy (26). Longitudinal and multi-site surveillance of a tumor's genetic profile is crucial for customized treatment of the primary malignancy and concomitant metastatic syndromes but requires tumor accessibility throughout the course of the disease. Repeated invasive tissue biopsy is not viable, especially in advanced cancer stage (27). In recent years, the vast potential of liquid-based biopsy as an alternative specimen for genomic analysis has been illustrated extensively (28–30). Circulating tumor cells and circulating cell-free tumor DNA in the body fluids emerge from the primary tumor and (micro-) metastatic lesions, thus capturing the tumor's spatial heterogeneity (31). As sampling is minimal-invasive, liquid-biopsy paves the way to real-time genotyping throughout the course of the disease (32). Various studies have already addressed and confirmed the informative value of MPE as a liquid biopsy specimen, especially in lung oncology (33–36). Pleural fluid´s *EGFR* mutation status was shown highly predictive of *EGFR*-tyrosine kinase inhibitor (TKI) efficacy in advanced NSCLC (37), the leading cause of global cancer related mortality (38). Still, working with liquid biopsies is challenging as the count of isolable neoplastic cells is variable and circulating tumor DNA is fragmented and greatly underrepresented compared to superimposed germ line DNA. Extremely sensitive assays are vital to capture rare mutations in an uncertain fraction of tumor DNA (39). Sanger sequencing, the current gold standard for clinical research sequencing, and next generation sequencing require at least 20% (40) and 2-6% (41) mutant alleles per sample, respectively. By contrast, droplet digital polymerase chain reaction (ddPCR) technology reaches a limit of detection (LOD) below 0,1% allelic frequencies in wildtype DNA-background (42). The input DNA is partitioned in up to 20.000 droplets followed by independent PCR amplification and fluorescence labeling for the target DNA, hence increasing the target signal-to-noise ratio.

2 Hypothesis

2.1 The diagnostic value of clinical data for MPE assessment

Pleural effusion often occurs as the first sign of an advanced malignancy. Fast and reliable identification of its causative primary tumor and the earliest possible start of the corresponding cancer therapy regimen is crucial for the patient´s outcome. Unfortunately, MPE diagnostics are protracted and inconclusive to a significant extent. Initial pleural fluid examination leaves the primary tumor undiagnosed in up to 40% of cases (43) and a substantial 15% remain unsolved despite further invasive thoracoscopic sampling (44). Time consuming diagnostics impair early tumor staging, therapy onset and thus patients' prognosis. Here arises the need for innovation in clinical MPE assessment. Some recent approaches consult blood and pleural fluid biomarkers (45), distinctive radiological criteria (46) and innovative imaging techniques (47).The aim of this thesis is to assess the value of common clinical information, such as lung function and laboratory data, for the differential diagnostics of MPE's etiology, especially its discriminative capacity for mesothelioma. The final objective is to create a clinical scoring system based upon parameters that significantly differ between patients with MPE due to a primary or metastatic pleural malignancy. Such diagnostic tool, based on clinical parameters obtained in daily practice, could be widely applicable for an introductory screening of patients presenting with MPE of unknown origin.

2.2 Mutational profiling of pleural fluid facilitates targeted MPE therapy

Mutational profiling of MPE could revolutionize its therapeutic management. Circulating pleural tumor DNA carries the genetic profile of MPE competence. The identification of attributable genetic alterations can authorize the application of corresponding biopharmaceutics. Within this project, MPE cell pellets and supernatants shall be assessed for *EGFR* and *KRAS* status. Both oncogenes contribute to MPE induction and both are druggable (18,21). TKIs against *EGFR*, such as gefitinib, have become the first-line treatment for NSCLC patients with sensitive EGFR mutations (exon 19 deletion (*EGFR* ex19del) and exon 21 L858R mutations). The progression-free survival is significantly improved compared to conventional chemotherapy (48). Several studies indicate the TKI- response of pleural metastasis similar to

its primary tumor (49). Gefitinib administered to NSCLC patients with MPE reduced the effusion volume by more than 50% for at least three months (50). Given the prevalence of *EGFR* mutations in MPE samples (median 34%) (51), this effect is plausible. Mutant *KRAS* was recently revealed as another actionable key promotor of MPE. Pharmacologic interception of oncogenic KRAS signaling is effective in halting MPE induction in mouse models (18). Still, the proposed genotype-phenotype link misses confirmation by human MPE sequencing studies. Available studies yield a mean of 20% *KRAS* mutation frequency (35,52–54), but this has to be taken as an underestimation and will be reviewed as a main part of this project. Although *KRAS* is the most frequently mutated oncogenic driver in NSCLC (55), *KRAS* mutations were not considered actionable so far and hence rarely looked at, in contrast to *EGFR* mutations. *KRAS* and *EGFR* were even considered mutually exclusive for the longest time (55). This presumption is currently revised. *KRAS* mutations might be acquired subsequent to dominant oncogenic driver mutations and coexist in the same tumor cell clone. Also, different driver mutations may be present in different tumor cells, establishing genetically heterogeneous subgroups (56). The multiclonality and multifocality of pleural malignancies explain the need of liquid-biopsy sampling for evaluation of the proposed *KRAS*-MPE link. A significant fraction of mutant *KRAS* might escape focal pleural biopsy. Further it should be noted that MPE sequencing is predominantly performed for NSCLC patients in the Asian population. The oncogene status of NSCLC differs markedly regarding geographics. Whereas *EGFR* mutations vary from 36-66% in lung adenocarcinoma in East Asia, they account for solely 12-14% in Caucasian population. This is reversed for *KRAS*, with a mutation frequency of 33-35% in western and 2-9% in Asian population (52). Such a biased cohort profile presumably leads to underestimation of overall mutant *KRAS* frequency. Moreover, liquid-based biopsy requires extremely sensitive sequencing approaches due to the fragmented and greatly underrepresented tumor DNA. Automated Sanger Sequencing trace analysis might miss *KRAS* mutations present at a low mutant allele frequency in superimposing wildtype traces (18). To guarantee an optimal detection rate for this project, MPE-derived cellular and cell-free DNA shall be tested with the extremely sensitive ddPCR technique.

3 Materials

Assays and kits:

ddPCR™ KRAS G12/G13 Screening Kit	Bio-Rad Laboratories Inc., Hercules, CA, USA
ddPCR™ KRAS Q61 Screening Kit	Bio-Rad Laboratories Inc., Hercules, CA, USA
ddPCR™ EGFR Exon 19 Deletions Screening Kit	Bio-Rad Laboratories Inc., Hercules, CA, USA
GenElute ™ Mammalian Genomic DNA Miniprep Kit	Sigma-Aldrich, St. Louis, MO, USA
QIAamp® Circulating Nucleic Acid Kit	QIAGEN, Hilden, Germany
Qubit™ dsDNA HS Assay Kit	Life Technologies, Carlsbad, CA, USA

Buffer and reagents:

Droplet Generation Oil for Probes	Bio-Rad Laboratories Inc., Hercules, CA, USA
PBS	NaCl 8 g, Na_2HPO_4 1.15 g, KH_2PO_4 0.2 g, H_2O to 1 L
TRIzol™ LS reagent	Thermo Fisher Scientific, Waltham, MA, USA

Lab equipment:

C1000 Touch™ Thermal Cycler with 96–Deep Well Reaction Module	Bio-Rad Laboratories Inc., Hercules, CA, USA
Eppendorf Model 5436 Thermomixer	Eppendorf AG, Hamburg, Germany
Hettich® MIKRO 200/200R Centrifuge	Hettich, Tuttlingen, Germany
Hettich® ROTANTA 460/460R Centrifuge	Hettich, Tuttlingen, Germany
Lauda MA6 Water bath incubator	Lauda, Lauda-Königshofen, Germany
Marienfeld Superior™ Counting chamber	Paul Marienfeld GmbH & Co. KG, Lauda- Königshofen, Germany
NanoDrop® ND-1000 Spectrophotometer	PEQLAB Biotechnologie GmbH, Erlangen, Germany
PX1™ PCR Plate Sealer	Bio-Rad Laboratories Inc., Hercules, CA, USA
QIAvac 24 Plus Vacuum System	QIAGEN, Hilden, Germany
Qubit™ 3 Fluorometer	Life Technologies, Carlsbad, CA, USA
QX100™ Droplet Generator	Bio-Rad Laboratories Inc., Hercules, CA, USA
QX100™ Droplet Reader	Bio-Rad Laboratories Inc., Hercules, CA, USA
Savant™ SpeedVac™ SPD120 Vaccum concentrator	Thermo Fisher Scientific, Waltham, MA, USA
ZEISS Axio Imager 2 Microscope	Zeiss, Jena, Germany

Consumables:

Corning® Syringe filters	Corning, Corning, NY, USA
ddPCR™ 96-Well Plates	Bio-Rad Laboratories Inc., Hercules, CA, USA
DG8™ Cartridges for QX100™ Droplet Generator	Bio-Rad Laboratories Inc., Hercules, CA, USA
DG8™ Cartridge Holder	Bio-Rad Laboratories Inc., Hercules, CA, USA
DG8™ Gaskets for QX100™ Droplet Generator	Bio-Rad Laboratories Inc., Hercules, CA, USA
EASYstrainer™ 40ym Cell strainer	Greiner Bio-One, Kremsmünster, Austria
Qubit® Assay tubes	Life Technologies, Carlsbad, CA, USA

Software:

GraphPad Prism 8.0	GraphPad Software, San Diego, CA, USA
QuantaSoft™ Analysis Pro Software	Bio-Rad Laboratories Inc., Hercules, CA, USA

Cell lines:

Cell line	Sequence variation	Tissue of origin
A549	Homozygous for KRAS p.Gly12Ser (c.34G>A)	Lung adenocarcinoma
NCl-H1568	Homozygous for TP53 p.His179Arg (c.536A>G)	Lymph node metastasis (Lung adenocarcinoma)
NCl-H3122	EML4-ALK gene fusion	Lung adenocarcinoma
NCl-H460	Homozygous for KRAS p.Gln61His (c.183A>T)	Lung large cell carcinoma

4 Methods

4.1 The MPE cohort

This research project was conducted in accordance with the Helsinki Declaration and was approved by the LMU Ethics Committee (623-15). Clinical data and biologic specimen were obtained by the Asklepios Biobank for Lung Diseases. All patients gave written informed consent a priori. The MPE cohort is represented by 45 patients that were treated at the Asklepios Medical Center Gauting between September 2015 and February 2017 because of conditions associated with pleural effusion formation. Baseline data obtained for each biobank donor were blinded patient identifier, clinical cancer diagnosis, sex and age, smoking status and date of intervention. Pre-interventional plethysmographic lung function tests and blood tests, including arterial blood gas analysis at ambient air, were enclosed. Figure 1 presents all clinical information available. Additional cancer registry query retrospectively provided the date of initial cancer diagnosis and the date of death. Unfortunately, survival data was censored as there was no follow-up scheduled for the biobank donors and cancer registry entries were incomplete. The MPE cohort was grouped according to effusion's etiology in patients with benign pleural effusion (BPE, *n* = 5), MPE due to mesothelioma (MESO, *n* = 12) and MPE due to a metastatic pleural malignancy (MET, *n* = 28) (Table 1). The latter group was further subdivided into patients with NSCLC (*n* = 18), including 16 patients with lung adenocarcinoma, and other metastatic cancer (otherCA, *n* = 10), precisely breast cancer (*n* = 4), small-cell lung carcinoma (*n* = 1), ovarian cancer (*n* = 2), Non-Hodgkin lymphoma (*n* = 2) and thymic carcinoma (*n* = 1). Pleural effusion samples were collected by pleurocentesis or during surgical intervention and provided together with their pathologic examination report.

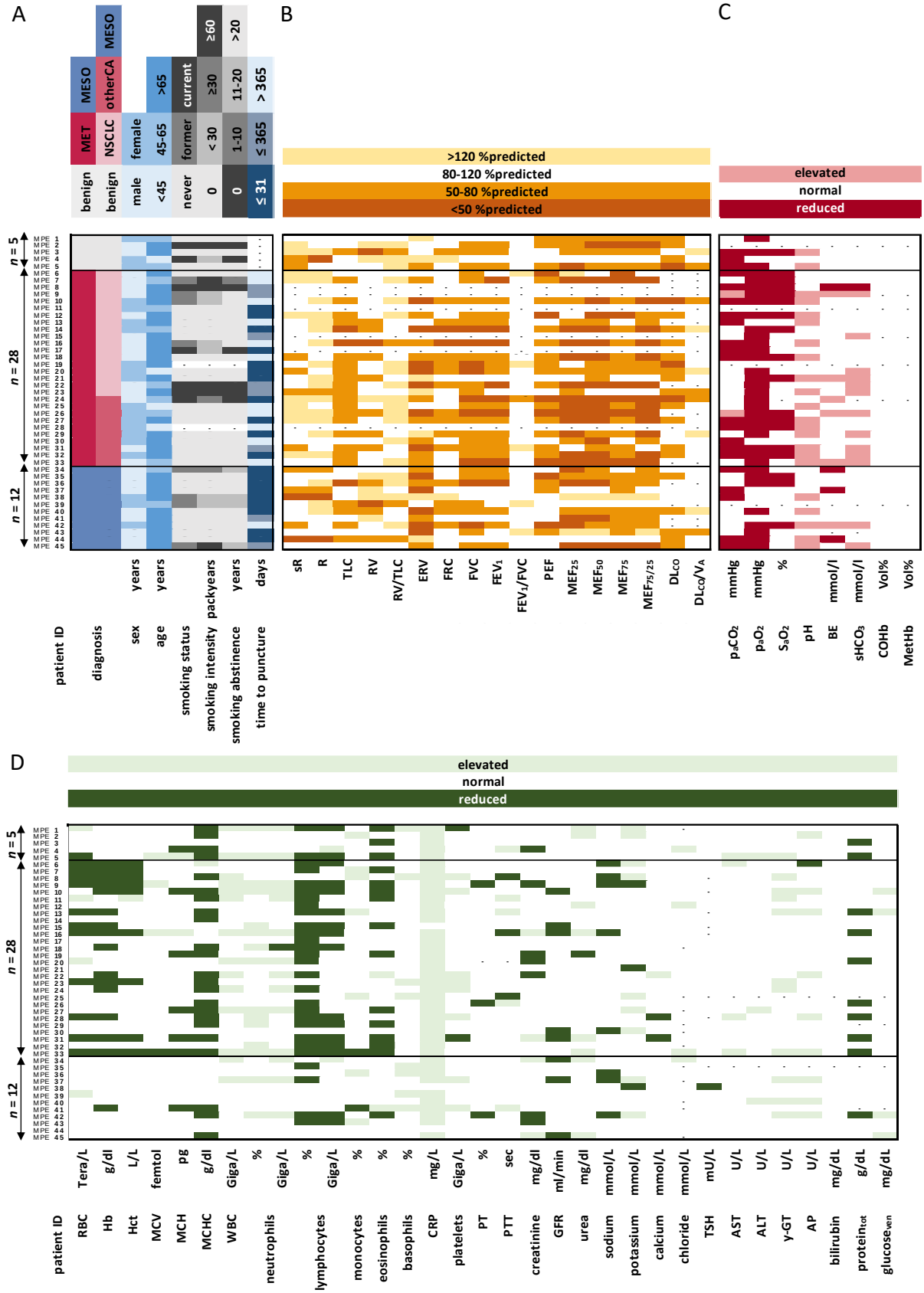
A
B
C
D
patient ID
diagnosis
sex
age
smoking status
smoking intensity
smoking abstinence
time to puncture
years
years
packyears
years
days
benign
benign
male
<45
never
0
0
≤ 31
MET
NSCLC
female
45-65
former
< 30
1-10
≤ 365
MESO
otherCA
>65
current
≥30
11-20
> 365
MESO
>20
≥60
>120 %predicted
80-120 %predicted
50-80 %predicted
<50 %predicted
sR
R
TLC
RV
RV/TLC
ERV
FRC
FVC
FEV1
FEV1/FVC
PEF
MEF25
MEF50
MEF75
MEF75/25
DLCO
DLCO/VA
elevated
normal
reduced
paCO2
paO2
SaO2
pH
BE
sHCO3
COHb
MetHb
mmHg
mmHg
%
mmol/l
mmol/l
Vol%
Vol%
n = 5
n = 28
n = 12
MPE 1
MPE 2
MPE 3
MPE 4
MPE 5
MPE 6
MPE 7
MPE 8
MPE 9
MPE 10
MPE 11
MPE 12
MPE 13
MPE 14
MPE 15
MPE 16
MPE 17
MPE 18
MPE 19
MPE 20
MPE 21
MPE 22
MPE 23
MPE 24
MPE 25
MPE 26
MPE 27
MPE 28
MPE 29
MPE 30
MPE 31
MPE 32
MPE 33
MPE 34
MPE 35
MPE 36
MPE 37
MPE 38
MPE 39
MPE 40
MPE 41
MPE 42
MPE 43
MPE 44
MPE 45
patient ID
RBC
Hb
Hct
MCV
MCH
MCHC
WBC
neutrophils
lymphocytes
monocytes
eosinophils
basophils
CRP
platelets
PT
PTT
creatinine
GFR
urea
sodium
potassium
calcium
chloride
TSH
AST
ALT
γ-GT
AP
bilirubin
proteintot
glucosefast
Tera/L
g/dl
L/L
femtol
pg
g/dl
Giga/L
%
Giga/L
%
Giga/L
%
%
%
%
mg/L
Giga/L
%
sec
mg/dl
ml/min
mg/dl
mmol/L
mmol/L
mmol/L
mmol/L
mU/L
U/L
U/L
U/L
U/L
mg/dL
g/dL
mg/dL

Figure 1 | Clinical information recorded for the MPE cohort
Color-coded pivot tables presenting all clinical data that has been listed at Biobank enrollment. Rows represent the individual patients and columns the clinical parameters. Undetermined information is denoted by a dash. *n*, number of patients; ID, identifier. (A) General features of the cohort, sorted by primary cancer, sex, age, smoking status and timespan between initial cancer diagnosis and pleurocentesis/intervention. BPE, benign pleural effusion (*n* = 5); MESO, mesothelioma (*n* = 12); MET, metastatic pleural malignancy (*n* = 28); NSCLC, non-small-cell lung carcinoma (*n* = 18); otherCA, other metastatic cancer (*n* = 12). (B) Lung function parameter (from left to right): sR, specific airway resistance; R, airway resistance; TLC, total lung capacity; RV, residual volume; ERV, expiratory reserve volume; FRC, functional residual capacity; FVC, forced vital capacity; FEV_1, forced expiratory volume in one second; FEV_1/FVC, Tiffeneau-Index; PEF, peak expiratory flow; MEF_{25}, mean expiratory flow at 25% of forced vital capacity; MEF_{50}, mean expiratory flow at 50% of forced vital capacity; MEF_{75}, mean expiratory flow at 75% of forced vital capacity; $MEF_{75/25}$, mean expiratory flow between 75% and 25% of forced vital capacity; DL_{co}, lung diffusion capacity for carbon monoxide; V_A, alveolar ventilation. (**C**) Arterial blood gas analysis at ambient air (from left to right): p_aCO_2, arterial partial pressure of carbon dioxide; p_aO_2, arterial partial pressure of oxygen; S_aO_2, arterial oxygen saturation; BE, base excess; $sHCO_3$, standard bicarbonate; COHb, carboxyhemoglobin; MetHb, methemoglobin. (**D**) Blood examination (from left to right): RBC, red blood cell count; Hb, hemoglobin; Hct, hematocrit; MCV, mean corpuscular volume; MCH, mean corpuscular hemoglobin; MCHC, mean corpuscular hemoglobin concentration; WBC, white blood cell count; CRP, C-reactive protein; PT, prothrombin time; PTT, partial thromboplastin time; GFR, glomerular filtration rate; TSH, thyroid stimulating hormone; AST, aspartate aminotransferase; ALT, alanine aminotransferase; y-GT, gamma-glutamyltransferase; AP, alkaline phosphatase; $protein_{tot}$, plasma total protein; $glucose_{ven}$, venous blood glucose.

Table 1 | The MPE cohort

Subgroups	Abbreviation	*n*
Benign pleural effusion	BPE	5
Malignant pleural effusion	**MPE**	**40**
Metastatic pleural malignancy	**MET**	**28**
Non-small-cell lung carcinoma	NSCLC	18
Other metastatic cancer	otherCA	10
Mesothelioma	**MESO**	**12**

n, number of patients

4.2 Clinical data analysis

The aim here was to determine the discriminative capacity of lung function and blood test parameters for MPE´s etiology. BPE wasn't included in the statistics due to the small group size. Statistical analysis was performed with GraphPad Prism Software 8.0. For each clinical parameter, the distribution of the unpaired groups MET and MESO was compared with the non-parametric Mann-Whitney test. If the group distribution significantly differed, receiver operating characteristic (ROC) analysis assessed the parameter's diagnostic ability as a binary classifier system for effusion´s etiology. Cut-off values predictive of mesothelioma were defined as the discrimination threshold was varied and applied on the MPE cohort. For each criterion met, patients were assigned two points. If a criterion wasn´t met, one point was calculated. Missing data was considered as zero points. The discriminative capacity of such a scoring system and its predictive value for mesothelioma were determined by ROC-analysis.

Group distribution was evaluated by the Mann-Whitney test. As a next step, three parameters were selected for the final score. Regarding lung function, test reliability was a major selection criterion. Spirometric measures depend on the patient´s active collaboration, raising statistical bias. Airway resistance (R) assessed by body plethysmography is least affected by test execution. The blood parameter arterial partial pressure of oxygen at ambient air (p_aO_2) and hemoglobin (Hb) are obtained by direct measurement. They are indicative of the blood oxygenation status and thus essential in lung oncology. R, p_aO_2 and Hb with their corresponding cut-off criteria, as determined earlier, were reapplied to the cohort. Patients with missing information were excluded. For each criterion met, one point was assigned. Then again ROC analysis was used to attest the performance of the emerging diagnostic classification model and a forecast value for mesothelioma was defined. Group distribution was evaluated by the Mann-Whitney test.

Additionally, each patient was diagnosed for: ventilatory and gas exchange disorder, anomalies of blood gas analysis such as oxygenation impairment and metabolic derangement, inflammation and immune dysregulation, coagulation disorder, renal dysfunction, electrolyte imbalances and hepatic or cholestatic impairment. Associations of such diagnostic patterns with MPE's etiology were evaluated by contingency analysis.

4.3 Molecular analysis of MPE

4.3.1 Processing of pleural fluid samples

Pleural fluid was centrifugated at 4 °C and 300 RPM for 10 min and the supernatant (SUP) was removed carefully. 50 ml of cell-free MPE SUP was stored at -20 °C. The pooled cells were mixed with 1 ml PBS buffer and Neubauer chamber was used to count the cells. 750 µl TRIzol LS reagent per 5-10 x 10^6 cells was added to the MPE cell pellet (CP). Tubes were stored at -20 °C until DNA extraction. Cellular DNA (cDNA) was isolated using the TRIzol LS reagent, following the manufacturer’s instruction. cDNA purification was performed with the GenElute Mammalian Genomic DNA Miniprep Kit and the NanoDrop spectrophotometer was used for cDNA quantification and quality check. cDNA was stored at -20 °C. MPE SUPs were further centrifuged at RT and 10000 RPM for 10 min and prefiltered with a 40 µm cell strainer to remove all cell debris and cryoprecipitates. Purification of the cell-free circulating DNA

(cfDNA) was performed with the QIAamp Circulating Nucleic Acid Kit and the QIAvac 24 Plus vacuum manifold according to the manufacturer's protocol: 'Purification of Circulating Nucleic Acids from 4 ml or 5 ml Serum or Plasma'. 5 ml SUP was used for extraction. To optimize the vacuum processing of the QIAamp Mini spin columns, MPE SUPs were filtered with a 0.45 µm and 0.20 µm syringe filter in a row before adding the binding Buffer ACB to the lysate. A maximum of 150 µl elution volume was used. cfDNA was quantified using the Qubit dsDNA HS (High Sensitivity) Assay Kit with the Qubit 3 Fluorometer. The assay is highly selective for double-stranded DNA over RNA and accurate for sample concentrations from 10 pg/µL to 100 ng/µL. cfDNA was stored at -20 °C.

4.3.2 *KRAS* and *EGFR* mutation detection with droplet digital PCR

ddPCR technology was used to detect MPE driver mutations in the paired CP-derived cDNA and SUP-derived cfDNA of 45 effusion samples. *KRAS* codon 12 and 13 mutations were tested with the ddPCR KRAS G12/G13 Screening Kit. It contains mutation detection assays for G12A, G12C, G12D, G12R, G12S, G12V and G13D point mutations. The ddPCR KRAS Q61 Screening Kit was used to screen the samples for the following *KRAS* mutations in codon 61: Q61K, Q61L, Q61R, Q61H 183A>T and Q61H 183A>C. The *EGFR* mutation status was determined using the ddPCR EGFR Exon 19 Deletions Screening Kit, which is validated for fifteen deletion mutations in exon 19 (2235_2252>AAT, 2235_2249del15, 2236_2250del15, 2238_2252>GCA, 2238_2255del18, 2239_2253>CAA, 2239_2251>C, 2239_2258>CA, 2239_2252>CA, 2239_2256del18, 2239_2248TTAAGAGAAG>C, 2239_2253del15, 2239_2247delTTAAGAGAA, 2240_2254del15 and 2240_2257del18). Each ddPCR screening multiplex assay combines various mutation detection assays with their reference assay in a ready-to-use primer-probe mix. Primers are labeled with competitive fluorescent probes for the mutant (Carboxyfluorescein (FAM)-labeled target assays) and wildtype allele (Hexachlorofluorescein (HEX)-labeled reference assay). All ddPCR mutation detection assays have been wet-lab validated down to a fractional abundance of 0,1% mutant DNA in the background of wildtype DNA in one well. This assumes an ideal assay and experimental performance with a droplet false positive ratio of zero. As the LOD predominately depends on the amount of amplifiable genome copies/sample loaded, all ddPCR reactions were performed on 200 ng cDNA and 20 ng cfDNA per well to create the conditions for an optimal LOD of 0,1%. The cDNA-input was

adjusted according to the spectrophotometric nucleic acid purity ratios. An adequate cDNA quality was assumed for a 260nm/230nm absorbance ratio between 2.0-2.2 and a 260nm/280nm ratio of 1.8. NCl-H3122 and NCl-H1568 cells were used as mutation-negative controls, A549 (*KRAS*^{G12S}) and NCl-H460 (KRAS^{Q61H}) as mutation-positive controls for *KRAS* G12/13 and Q61 mutations, respectively. The Gauting locoregional lung adenocarcinoma donors (GLAD) cohort (57) provided the positive (ASK152) and negative (ASK059) controls for *EGFR* mutation testing . An *EGFR* ex19del mutation has been confirmed by Sanger sequencing in both lung adenocarcinoma samples. The mutation-negative control wells were loaded equal to the sample concentration for correct estimation of the false-positive rate. Several no template control wells with nuclease-free water, were added to preclude environmental contamination. The ddPCR reactions were performed according to the corresponding screening kit protocols. Each ddPCR reaction mix contained the 1X multiplex assay, 1X ddPCR supermix for probes (no UTP) and template DNA, adjusted to a final volume of 20µl with nuclease-free water. The reaction mix was loaded into the sample wells of a DG8 cartridge, then the oil wells were loaded with 70 µl droplet generation oil for probes. The QX100 droplet generator emulsified and partitioned each sample in up to 20.000 droplets. Droplets were transferred on a 96-well plate and sealed with the PX1 PCR plate sealer. The endpoint PCR was performed on the C1000 Touch thermal cycler according to following conditions (ramp rate 2 °C/sec): 95 °C for 10 min, 40 cycles of 94 °C for 30 sec, 55 °C for 1 min, and 98 °C for 10 min. After thermal cycling, the sealed plate was placed in the QX100 droplet reader. Fluorescence readings were measured for each droplet in two channels (Ch): Ch1 FAM (target assay) and Ch2 HEX (reference assay). After data acquisition, the experiment was analyzed with the QuantaSoft Analysis Pro software. Fluorescent thresholds were set manually, based on the control wells' fluorescent amplitudes in the 2D-scatterplot. Droplets were designated in four clearly separated clusters: double negative (Ch1-/Ch2-) droplets (containing no specific DNA template), wildtype only (Ch1+/Ch2-) droplets, mutant only (Ch1+/Ch2+) droplets and double positive (Ch1+/Ch2+) droplets (containing the wildtype and mutant template in the same droplet). Using the 1D-scatterplot, the Ch1 threshold was further adjusted to sit just below the positive cluster in the mutation positive control well, thus avoiding overestimation of false positives. A minimum of three positive droplets (Poisson's law) and the assay's LOD were applied for confidently calling a sample mutant. To yield absolute mutation percentages, data were normalized by accepted droplet count and applied to the formula:

$$\text{Mutant genome copies (\%)} = \frac{n\ (\text{FAM positive})}{n\ (\text{FAM positive}) + n\ (\text{HEX positive})} \times 100;\ n = \text{number of droplets.}$$

5 Results

5.1 Lung function and blood test parameters predict MPE's etiology

The distribution of the following 19 parameters turned out to be significantly distinct between the groups MET and MESO: specific airway resistance (sR), airway resistance (R), forced vital capacity (FVC), forced expiratory volume in one second (FEV_1), peak expiratory flow (PEF), maximal expiratory flow at 75% of forced vital capacity (MEF_{75}), maximal expiratory flow at 50% of forced vital capacity (MEF_{50}), mean expiratory flow between 75% and 25% of forced vital capacity ($MEF_{75/25}$), lung diffusion capacity for carbon monoxide (DL_{CO}), arterial partial pressure of oxygen at ambient air (p_aO_2), arterial oxygen saturation at ambient air (S_aO_2), hemoglobin (Hb), red blood cell count (RBC), hematocrit (Hct), relative lymphocyte count ($lymphocytes_{rel}$), C-reactive protein (CRP), urea, calcium and total plasma protein ($protein_{tot}$) (Figure 2, Table 2). Each parameter's discriminative power for mesothelioma was determined and predictive threshold values were defined (table 3). A pilot score emerging out of these nineteen parameters (Figure 3) provides a diagnostic sensitivity of 83.33% and specificity of 89.29% for mesothelioma. Applied on the MPE cohort, 87.50% of MPE patients were matched true etiology. The Mesothelioma Score (Figure 4) only considers R, paO_2 and Hb. The score promises to predict mesothelioma with a sensitivity of 81.82% and a specificity of 95.24%, if two out of the three distinctive criteria are met. Thereby, 29 out of 32 patients with MPE were correctly diagnosed with a primary or metastatic pleural malignancy.

Moreover, suffering from wet pleural carcinomatosis appears to be related with a restrictive ventilatory defect, pulmonary gas exchange disorder, moderate or severe hypoxemia, anemia, erythropenia and relative lymphopenia (Table 4, Figure 5).

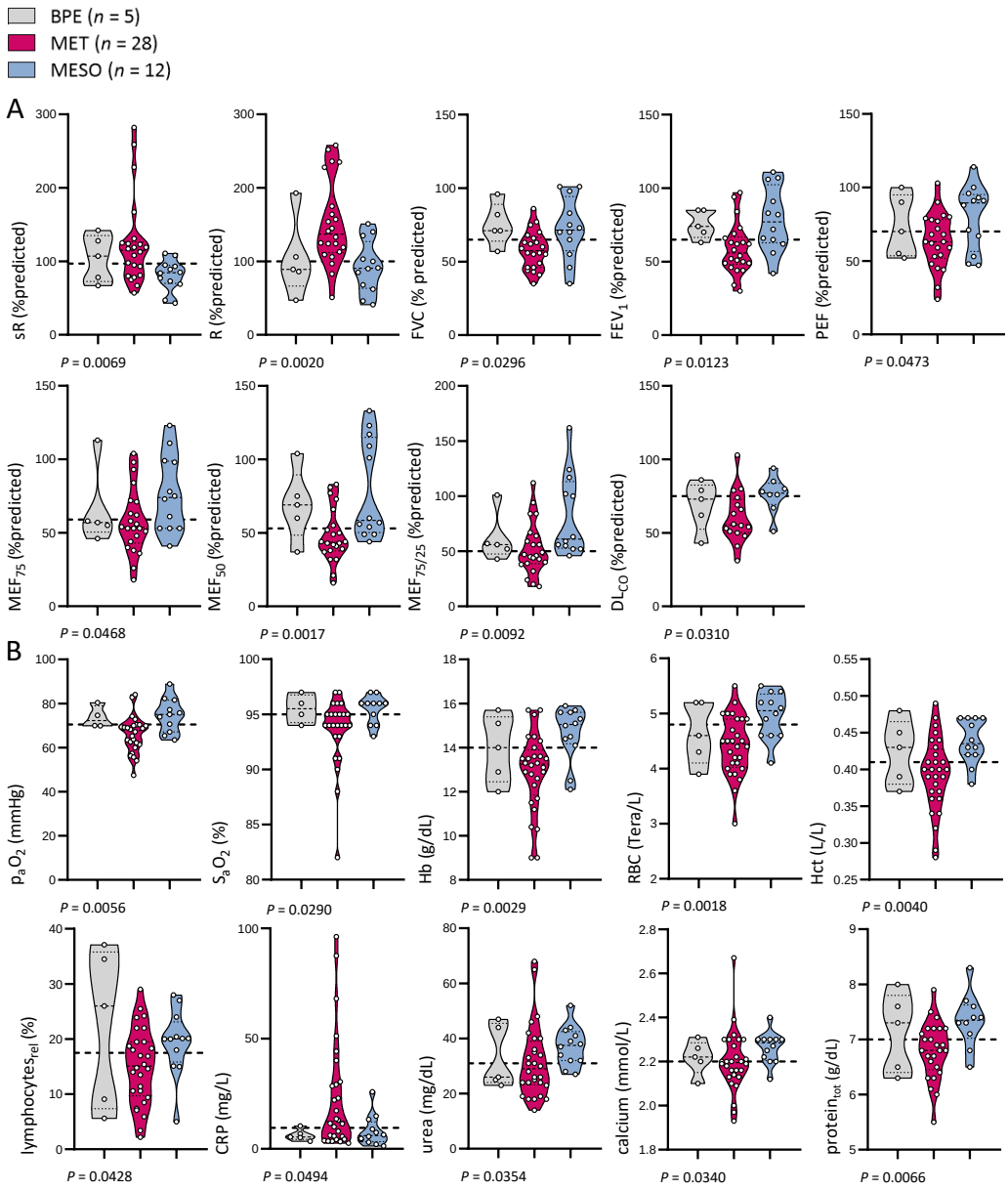

Figure 2 | Lung function and blood test parameters differ according to MPE's etiology
Presented are lung function and blood test parameters that demonstrate a significantly different distribution for the groups metastatic pleural malignancy (MET) and mesothelioma (MESO). Data are given as raw data points (circles) and violin plots with median (thick dashed lines), quartiles (thin dotted lines) and bilateral rotated Kernel density plots. Parameters are shown with predictive cut-off values for mesothelioma as depicted by the dashed line. *n*, number of patients; *P*, probability, Mann-Whitney test. The group of benign pleural effusion (BPE) is only illustrated for integrity. (A) Lung function parameters (from left to right): sR, specific airway resistance; R, airway resistance; FVC, forced vital capacity; FEV_1, forced expiratory volume in one second; PEF, peak expiratory flow; MEF_{75}, maximal expiratory flow at 75% of forced vital capacity; MEF_{50}, maximal expiratory flow at 50% of forced vital capacity; $MEF_{75/25}$, mean expiratory flow between 75% and 25% of forced vital capacity; DL_{CO}, lung diffusion capacity for carbon monoxide. (B) Blood test parameters (from left to right): p_aO_2, arterial partial pressure of oxygen at ambient air; S_aO_2, arterial oxygen saturation; Hb, hemoglobin; RBC, red blood cell count; Hct, hematocrit; $lymphocytes_{rel}$, relative lymphocyte count; CRP, C-reactive protein; $protein_{tot}$, total plasma protein.

A

Parameter	Cut-off	
sR	< 97	%predicted
R	≤ 100	%predicted
FVC	≥ 65	%predicted
FEV_1	≥ 65	%predicted
PEF	≥ 70	%predicted
MEF_{75}	> 50	%predicted
MEF_{50}	> 53	%predicted
$MEF_{75/25}$	> 50	%predicted
DL_{CO}	> 75	%predicted
p_aO_2	> 70	mmHg
S_aO_2	> 95	%
Hb	> 14	g/dL
RBC	> 4.8	Tera/L
Hct	> 0.41	L/L
$Lymphocytes_{rel}$	> 17.5	%
CRP	< 9.5	mg/L
Urea	> 31.0	mg/dL
Calcium	> 2.21	mmol/L
$Protein_{tot}$	> 7.0	g/dL

Criterion	Points
Met	2
Not met	1
Not available	0

B

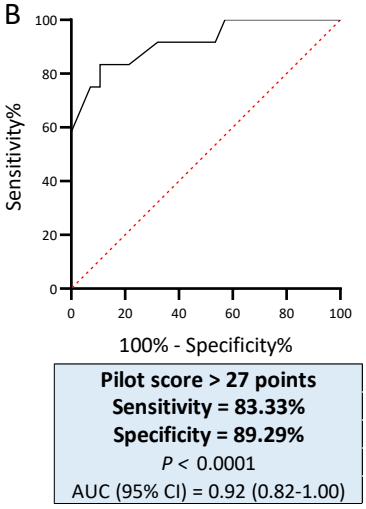

C

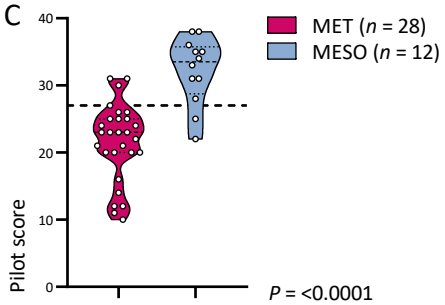

Figure 3 | Clinical parameters predict the etiology of MPE

Lung function and laboratory parameters form a binary classifier tool for the diagnosis of mesothelioma induced MPE. (A) Parameter compilation of the score with predictive cut-off values for mesothelioma and application instructions (from top to buttom): sR, specific airway resistance; R, airway resistance; FVC, forced vital capacity; FEV_1, forced expiratory volume in one second; PEF, peak expiratory flow; MEF_{75}, maximal expiratory flow at 75% of forced vital capacity; MEF_{50}, maximal expiratory flow at 50% of forced vital capacity; $MEF_{75/25}$, mean expiratory flow between 75% and 25% of forced vital capacity; DL_{CO}, lung diffusion capacity for carbon monoxide; p_aO_2, arterial partial pressure of oxygen at ambient air; S_aO_2, arterial oxygen saturation; Hb, hemoglobin; RBC, red blood cell count; Hct, hematocrit; $lymphocytes_{rel}$, relative lymphocyte count; CRP, C-reactive protein; $protein_{tot}$, total plasma protein. (B) Receiver operating characteristic (ROC) curve, illustrating the diagnostic ability of the pilot score as its discrimination threshold is varied. AUC (95% CI), area under the curve stated with 95% confidence interval; *P*, probability, ROC analysis. (C) Pilot score applied on the MPE cohort. Calculated points are illustrated as raw data points (circles) and violin plots with median (thick dashed lines), quartiles (thin dotted lines) and bilateral rotated Kernel density plots. The divisive score value is depicted by the dashed line. *n*, number of patients; *P*, probability, Mann-Whitney test; MET, metastatic pleural malignancy; MESO, mesothelioma.

Table 2 | Distinct parameter distribution according to MPE's etiology

Diagnosis			**BPE**	**MET**	**MESO**	*P*
n			5	28	12	
Lung function parameters						
	Abbreviation	Unit	Mean ± SD			
Specific airway resistance	sR	%predicted	104.40 ± 31.91	124.50 ± 59.72	81.17 ± 21.07	0.0069
Airway resistance	R	%predicted	104.20 ± 54.14	151.30 ± 57.34	92.67 ± 35.75	0.0020
Forced vital capacity	FVC	%predicted	75.40 ± 14.54	57.95 ± 12.81	72.67 ± 21.05	0.0296
Forced expiratory volume in one second	FEV_1	%predicted	75.40 ± 9.60	58.82 ± 17.17	78.58 ± 21.96	0.0123
Peak expiratory flow	PEF	%predicted	73.40 ± 21.16	63.73 ± 18.70	79.92 ± 22.11	0.0473
Mean expiratory flow at 75% of FVC	MEF_{75}	%predicted	65.80 ± 26.81	57.95 ± 22.14	76.50 ± 26.10	0.0468
Mean expiratory flow at 50% of FVC	MEF_{50}	%predicted	69.00 ± 24.32	48.09 ± 18.14	79.33 ± 33.98	0.0017
Mean expiratory flow between 75% and 25% of FVC	$MEF_{75/25}$	%predicted	61.80 ±22.60	52.77 ± 23.89	82.33 ± 37.54	0.0092
Lung diffusion capacity for carbon monoxide	DL_{CO}	%predicted	68.60 ± 16.80	60.81 ± 17.46	75.88 ± 12.71	0.0310
Blood test parameters						
	Abbreviation	Unit	Mean ± SD			
Arterial partial pressure of oxygen	p_aO_2	mmHg	73.73 ± 4.96	66.00 ± 8.22	74.68 ± 7.75	0.0056
Oxygen saturation	S_aO_2	%	95.50 ± 1.29	93.52 ± 3.20	95.45 ± 1.29	0.0290
Hemoglobin	Hb	g/dL	13.94 ± 1.52	12.91 ± 1.76	14.65 ± 1.23	0.0029
Red blood cell count	RBC	Tera/L	4.64 ± 0.57	4.41 ± 0.54	4.97 ± 0.42	0.0018
Hematocrit	Hct	L/L	0.42 ± 0.04	0.39 ± 0.05	0.44 ± 0.03	0.0040
Relative lymphocyte count	$lymphocytes_{rel}$	%	22.46 ± 14.44	15.12 ± 6.88	19.39 ± 6.05	0.0428
C-reactive protein	CRP	mg/L	6.22 ± 2.63	23.15 ± 25.55	8.14 ± 6.98	0.0494
Urea	-	mg/dL	33.00 ± 11.51	31.61 ± 13.27	37.25 ± 7.20	0.0354
Calcium	-	mmol/L	2.22 ± 0.08	2.20 ± 0.14	2.26 ± 0.07	0.0340
Total plasma protein	$protein_{tot}$	g/dL	7.14 ± 0.72	6.80 ± 0.52	7.34 ± 0.49	0.0066

BPE, benign pleural effusion; MESO, mesothelioma; MET, metastatic pleural malignancy; *n*, number of patients; *P*, probability, Mann-Whitney test.

Table 3 | Clinical parameters as binary classifiers for mesothelioma

Lung function parameters							
	Abbreviation	AUC (95% CI)	*P*	Cut-off	Sen (%)	Spe (%)	LR
Specific airway resistance	sR	0.78 (0.63-0.93)	0.0081	< 97% predicted	83.33	63.64	2.29
Airway resistance	R	0.81 (0.66-0.97)	0.0028	≤ 100% predicted	66.76	86.36	5.50
Forced vital capacity	FVC	0.73 (0.53-0.93)	0.0306	≥ 65% predicted	75.00	72.73	2.75
Forced expiratory volume in one second	FEV_1	0.76 (0.58-0.94)	0.0136	≥ 65% predicted	75.00	72.73	2.75
Peak expiratory flow	PEF	0.71 (0.51-0.91)	0.0475	≥ 70% predicted	66.67	63.64	1.83
Mean expiratory flow at 75% of FVC	MEF_{75}	0.71 (0.53-0.89)	0.0475	> 59% predicted	66.67	63.64	1.83
Mean expiratory flow at 50% of FVC	MEF_{50}	0.82 (0.68-0.96)	0.0025	> 53% predicted	75.00	72.73	2.75
Mean expiratory flow between 75% and 25% of FVC	$MEF_{75/25}$	0.77 (0.61-0.93)	0.0105	> 50% predicted	91.67	59.09	2.24
Lung diffusion capacity for carbon monoxide	DL_{CO}	0.77 (0.57-0.97)	0.0321	> 75% predicted	75.00	81.25	4.00
Blood test parameters							
	Abbreviation	AUC (95% CI)	*P*	Cut-off	Sen (%)	Spe (%)	LR
Arterial partial pressure of oxygen	p_aO_2	0.79 (0.62-0.95)	0.0068	> 70 mmHg	72.73	84.62	4.73
Oxygen saturation	S_aO_2	0.73 (0.55-0.91)	0.0332	> 95 %	63.64	80.00	3.18
Hemoglobin	Hb	0.79 (0.63-0.96)	0.0038	> 14.0 g/dL	83.33	78.57	3.89
Red blood cell count	RBC	0.80 (0.66-0.95)	0.0026	> 4.8 Tera/L	66.67	71.43	2.33
Hematocrit	Hct	0.78 (0.64-0.93)	0.0050	> 0.41 L/L	83.33	71.43	2.92
Relative lymphocyte count	$lymphocytes_{rel}$	0.70 (0.53-0.88)	0.0432	> 17.5 %	75.00	60.71	1.91
C-reactive protein	CRP	0.70 (0.53-0.87)	0.0497	< 9.5 mg/L	75.00	60.71	1.91
Urea	-	0.71 (0.56-0.87)	0.0361	> 31.0 mg/dL	83.33	60.71	2.12
Calcium	-	0.71 (0.55-0.88)	0.0361	> 2.2 mmol/L	75.00	64.29	2.10
Total plasma protein	$protein_{tot}$	0.79 (0.62-0.96)	0.0081	> 7.0 g/dL	80.00	68.00	2.50

AUC (95% CI), area under the curve stated with 95% confidence interval; LR; likelihood ratio; *P*, probability, Receiver operating characteristic analysis; Sen (%), sensitivity (%); Spe (%), specificity (%).

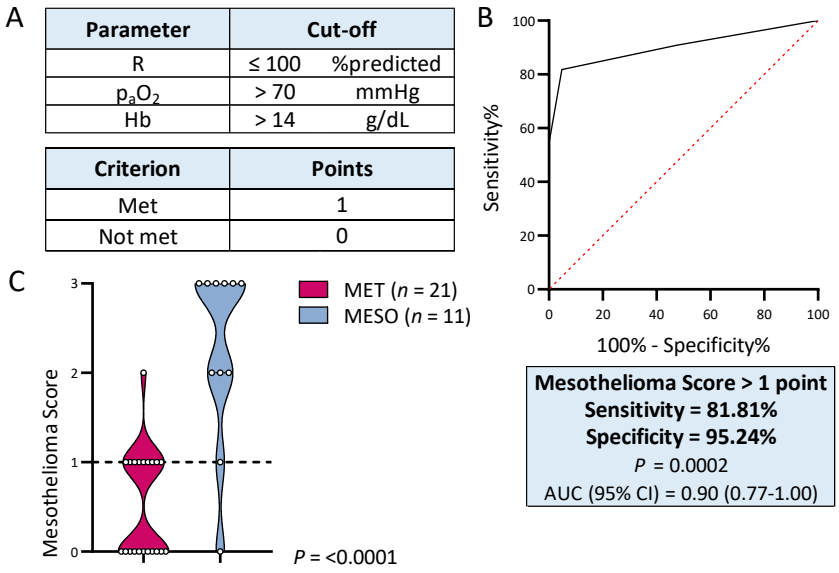

Figure 4 | The Mesothelioma Score
Presented is the Mesothelioma Score, a diagnostic screening tool for patients with MPE of unknown origin. (A) Clinical parameters with predictive cut-off values for mesothelioma and application instructions. R, airway resistance; p_aO_2, arterial partial pressure of oxygen at ambient air; Hb, hemoglobin. (B) Receiver operating characteristic curve (ROC), illustrating the diagnostic ability of the Mesothelioma Score as its discrimination threshold is varied. AUC (95% CI), area under the curve stated with 95% confidence interval; *P*, probability, ROC analysis. (C) Mesothelioma Score applied on the MPE cohort (patients with missing data were excluded). Calculated points are illustrated as raw data points (circles) and violin plots with median (thick dashed lines), quartiles (thin dotted lines) and bilateral rotated Kernel density plots. The divisive score value is depicted by the dashed line. *n*, number of patients; *P*, probability, Mann-Whitney test; MET, metastatic pleural malignancy, MESO, mesothelioma.

Table 4 | Characteristic diagnoses of patients with wet pleural carcinomatosis

	Diagnostic criteria	*P*
Restrictive ventilatory defect (58)	TLC < 80% predicted and FEV_1/FVC > 70%	0.0084
Pulmonary gas exchange disorder (58)	DL_{CO} < 75%	0.0215
Moderate or severe hypoxemia (59)	p_aO_2 < 70%	0.0252
Anemia	Hb < 12 g/dL (f) or < 14 g/dL (m) [1]	0.0122
Erythropenia	RBC < 4.1 Tera/L (f) or < 4.5 Tera/L (m) [1]	0.0170
Relative lymphopenia (60)	Lymphocytes < 20%	0.0108

DL_{CO}, diffusion capacity of the lung for carbon; f, female; FEV_1/FVC, Tiffeneau-Index; Hb, hemoglobin; m, male; *P*, probability, Fisher´s exact test; p_aO_2, arterial partial pressure of oxygen; RBC, red blood cell count; TLC, total lung capacity.

[1] according to the laboratory reference range

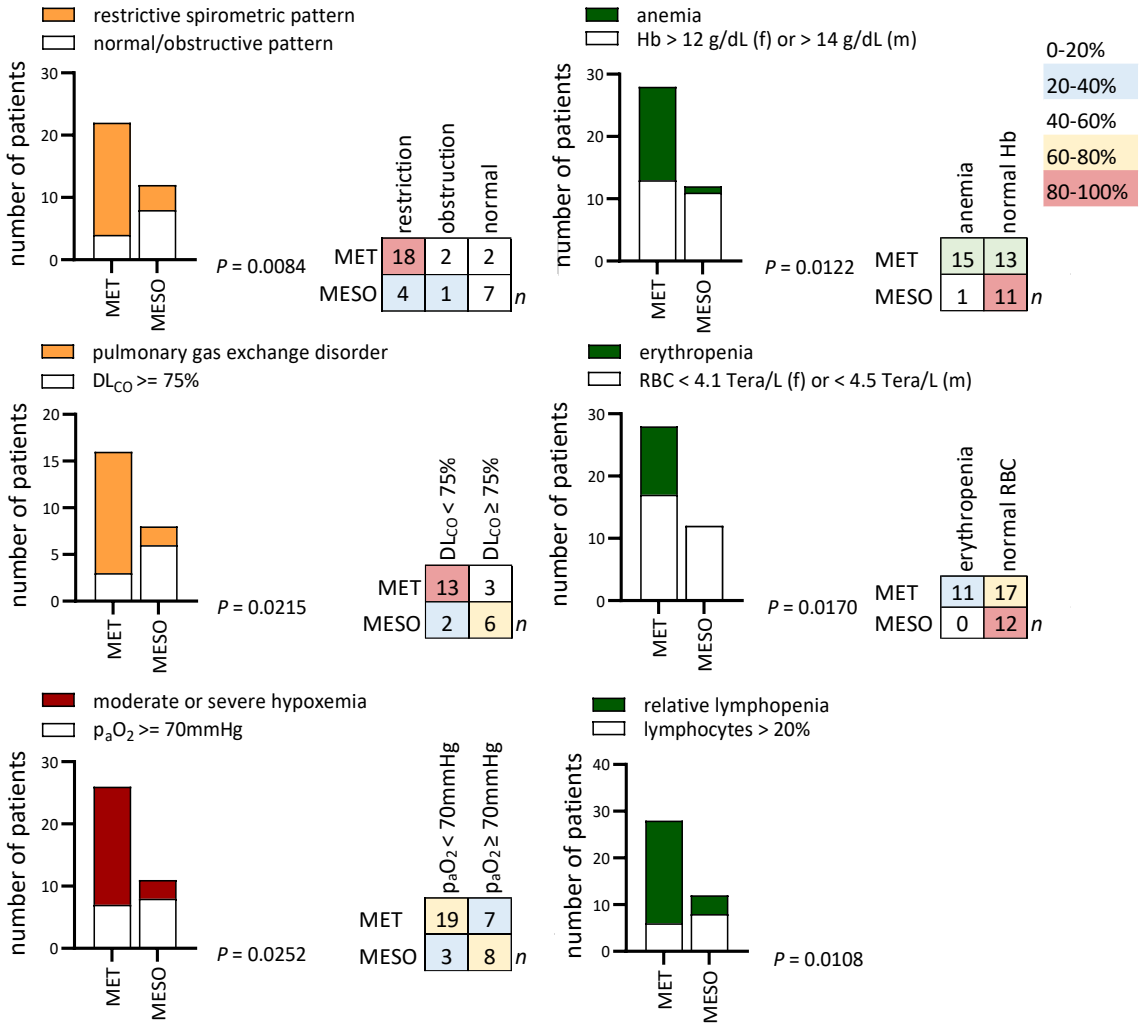

Figure 5 | Diagnostic patterns associated with MPE's etiology
Wet pleural carcinomatosis is associated with distinctive diagnostic patterns as illustrated by bar graphs and crosstabulations. DL_{CO}, lung diffusion capacity for carbon monoxide; MESO, mesothelioma; MET, metastatic pleural malignancy *n*; number of patients; *P*, Fisher's exact test; p_aO_2, arterial partial pressure of oxygen; RBC, red blood cell count.

5.2 *KRAS* and *EGFR* mutation status of the MPE cohort

MPE cohort's pleural effusion samples were divided by their CPs and SUPs and respectively assessed for *KRAS* mutations in codon 12/13 and codon 61, as well as *EGFR* ex19del mutations using ddPCR multiplex screening assays. Figure 6 charts the ddPCR 2D fluorescence amplitude plots of all mutant MPE samples divided by their CP- and SUP-run and visualizes the fractional abundance of mutant genome copies detected, respectively. Data analysis was performed in accordance with the wet-lab validated LOD of ddPCR mutation detection assays (0,1%). One patient with a pathologically diagnosed benign pleural effusion resulted *KRAS* G12/13 mutant (0.15% mutant genome copies in the cell pellet). For that patient, the serum marker neuron-

specific enolase (NSE) and pro-gastrin-releasing-peptide (pro-GRP) were tested positive, indicative of small-cell lung carcinoma. Due to the missing follow-up, this suspicion could not be verified. *KRAS* mutations were detected for 17 patients with MPE (42.50%). In five of the 40 paired samples, CP and SUP were both positive for *KRAS* mutation. In nine cases *KRAS* mutations were only detected in the CP and in three cases only in the SUP. Testing either the CP or SUP would have detected 14 (82.35%) and eight of the 17 (47.06 %) *KRAS* mutations, respectively. Twelve patients with a metastatic disease (42.85%) and five mesothelioma patients (41.67%) were *KRAS* mutant. The *KRAS* mutation frequency of NSCLC patients was 33.33%. Amongst all patients with *KRAS* mutations, eight had a codon 61 mutation (47.06%) and nine had a mutation in codon 12/13 (52.94%). *EGFR* ex19del mutations were confirmed for five patients with MPE (12.50%). Two effusion samples were *EGFR* mutant for both CP and SUP, and in three cases the mutant oncogene was only detected in the CP. Testing solely the SUP would have revealed only 40.00% of the *EGFR* mutations. Three NSCLC patients (16.67%) and one mesothelioma patient (8.33%) were *EGFR* mutant. Overall, 55.00% of MPE patients were assessed oncogene mutant. Figure 7A and Table 5 present a summary of the MPE cohort's mutation status. Mutations were detected in 86,36% of MPE CPs and 45.45% of MPE SUPs. CPs and SUPs differed significantly regarding mutation detection rate (P = 0.0097) and detectable mutation allele fraction (P = 0.0372, 10.89% mean ± 20.67 SD for CPs, 7.67 % mean ± 18.73 SD for SUPs) (Figure 7B).

I

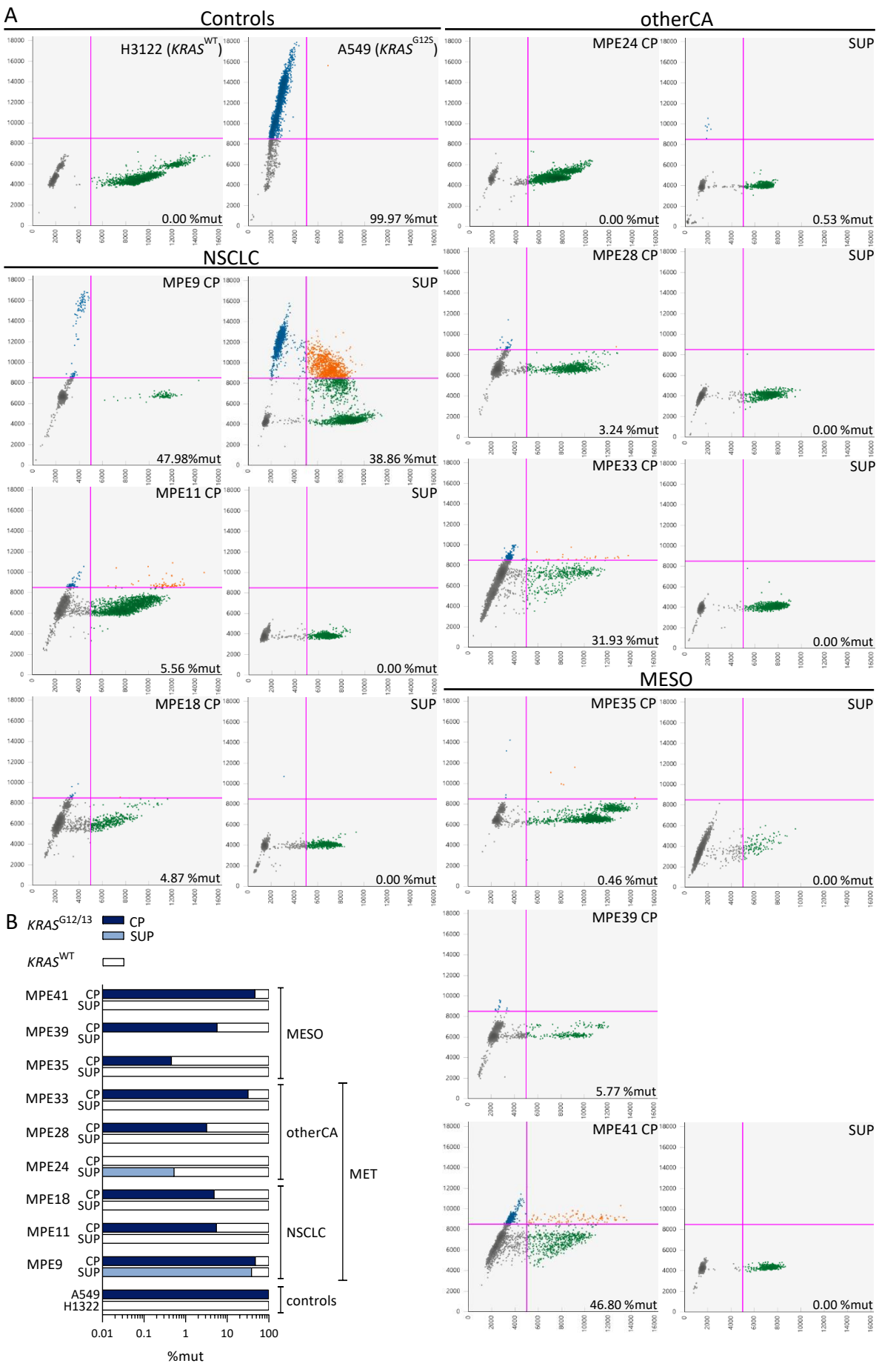
A
Controls
H3122 (KRAS^WT)
0.00 %mut
A549 (KRAS^G12S)
99.97 %mut
NSCLC
MPE9 CP
47.98%mut
SUP
38.86 %mut
MPE11 CP
5.56 %mut
SUP
0.00 %mut
MPE18 CP
4.87 %mut
SUP
0.00 %mut
otherCA
MPE24 CP
0.00 %mut
SUP
0.53 %mut
MPE28 CP
3.24 %mut
SUP
0.00 %mut
MPE33 CP
31.93 %mut
SUP
0.00 %mut
MESO
MPE35 CP
0.46 %mut
SUP
0.00 %mut
MPE39 CP
5.77 %mut
MPE41 CP
46.80 %mut
SUP
0.00 %mut
B
KRAS^G12/13
CP
SUP
KRAS^WT
MPE41
MPE39
MPE35
MPE33
MPE28
MPE24
MPE18
MPE11
MPE9
A549
H1322
MESO
otherCA
NSCLC
controls
MET
0.01
0.1
1
10
100
%mut

II

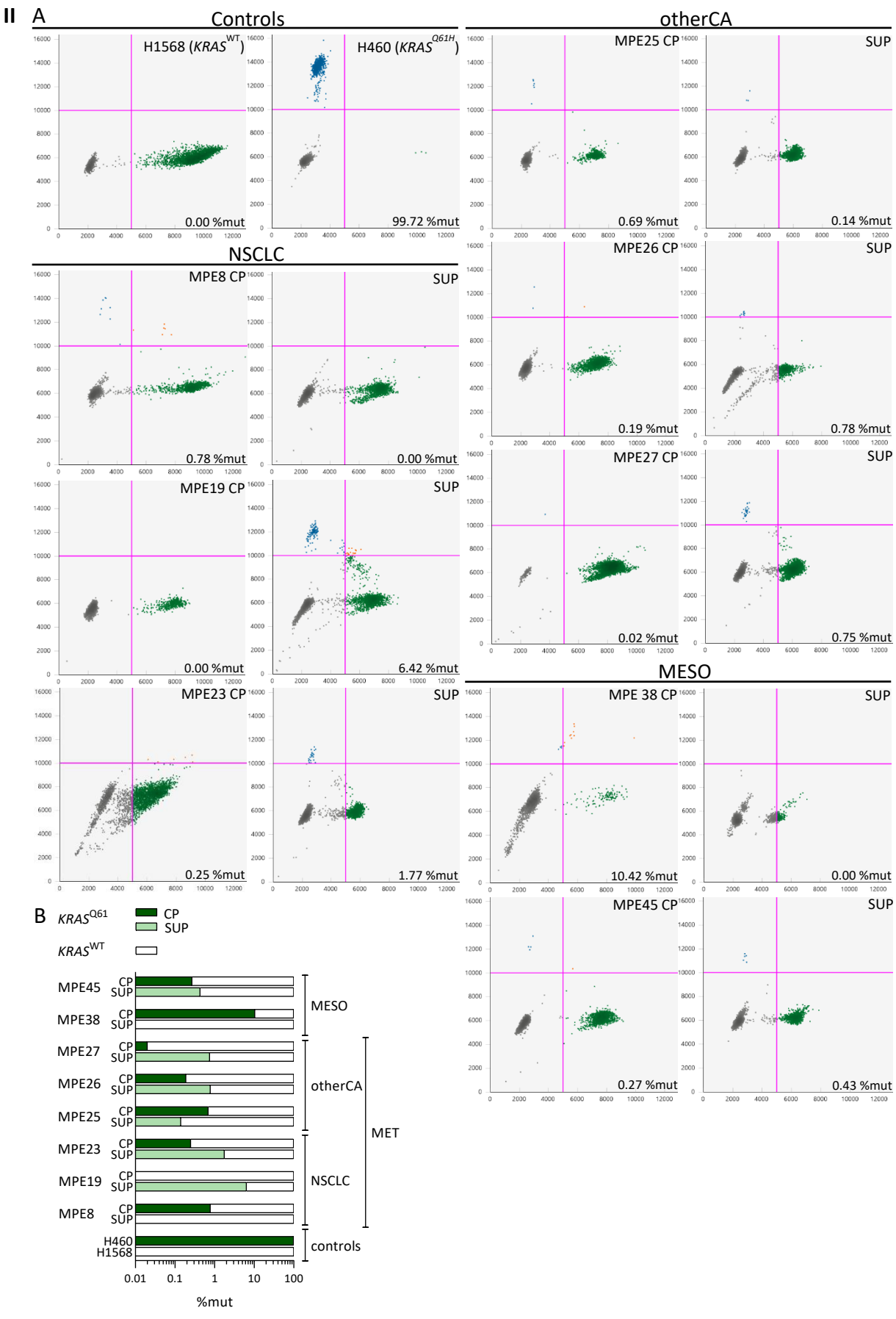
A
Controls
otherCA
H1568 (KRAS^WT)
H460 (KRAS^Q61H)
0.00 %mut
99.72 %mut
MPE25 CP
SUP
0.69 %mut
0.14 %mut
NSCLC
MPE8 CP
SUP
0.78 %mut
0.00 %mut
MPE26 CP
SUP
0.19 %mut
0.78 %mut
MPE19 CP
SUP
0.00 %mut
6.42 %mut
MPE27 CP
SUP
0.02 %mut
0.75 %mut
MESO
MPE23 CP
SUP
0.25 %mut
1.77 %mut
MPE 38 CP
SUP
10.42 %mut
0.00 %mut
MPE45 CP
SUP
0.27 %mut
0.43 %mut
B
KRASQ61
CP
SUP
KRASWT
MPE45
MPE38
MPE27
MPE26
MPE25
MPE23
MPE19
MPE8
H460
H1568
MESO
otherCA
NSCLC
controls
MET
0.01
0.1
1
10
100
%mut

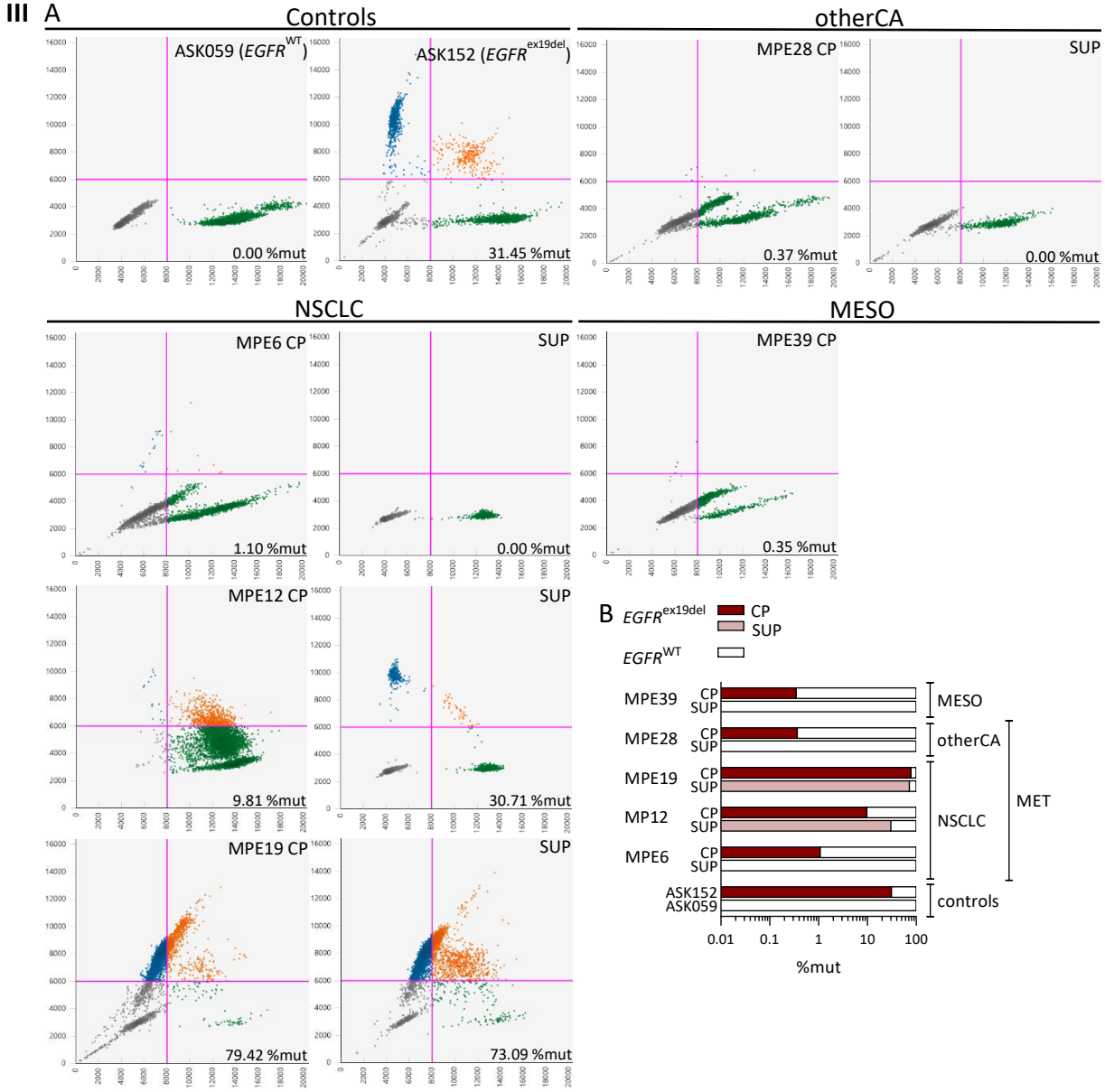

Figure 6 | Oncogene mutant MPE samples detected by droplet digital PCR

Pleural fluid cell pellets (CP) and supernatants (SUP) were subjected to droplet digital PCR (ddPCR) for the detection of KRAS mutations in codon 12/13 ($KRAS^{G12/13}$) (I) and codon 61 ($KRAS^{Q61}$) (II), as well as EGFR exon 19 deletion mutations ($EGFR^{ex19del}$) (III). NCI-H3122 ($KRAS^{WT}$)/A549 ($KRAS^{G12S}$), NCI-H1568 ($KRAS^{WT}$)/NCI-H460 ($KRAS^{Q61H}$) cells and the GLAD cohort (57)-derived lung adenocarcinoma samples ASK059 ($EGFR^{WT}$)/ASK059 ($EGFR^{ex19del}$) were used as controls, respectively. ddPCR data was analyzed with Quantasoft. MESO, mesothelioma; MET, metastatic pleural malignancy; MPE number, patient identifier for the MPE cohort; NSCLC, non-small-cell lung carcinoma; otherCA, other metastatic cancer. (A) ddPCR 2D-scatterplots of MPE patients that were detected *KRAS* G12/13 (IA), *KRAS* Q61 (IIA) and *EGFR* ex19del (IIIA) mutant. Single-well data for mutant DNA detection in wildtype DNA background. The multiplex mutation detection assay (Carboxyfluorescein (FAM)-labeled, channel 1) was duplexed with the corresponding wildtype reference assay (Hexachlorofluorescein (HEX)-labeled, channel 2); x-axis: channel 1 fluorescence amplitude, y-axis: channel 2 fluorescence amplitude. Designation of the droplets as double negative (gray), FAM single positive (blue), HEX single positive (green) and double positive (orange, positive for FAM and HEX in the same droplet) by manual thresholding based on their fluorescence amplitudes (pink grits). The percentage of mutant genome copies (%mut) is stated in the bottom right; calculation of %mut: *n* (FAM positive) / (*n* (FAM positive) + *n* (HEX positive)) * 100, *n* = number of droplets. (B) Summary of absolute mutation percentages for *KRAS* G12/13 (IB), *KRAS* Q61 (IIB) and *EGFR* ex19del mutations (IIIB).

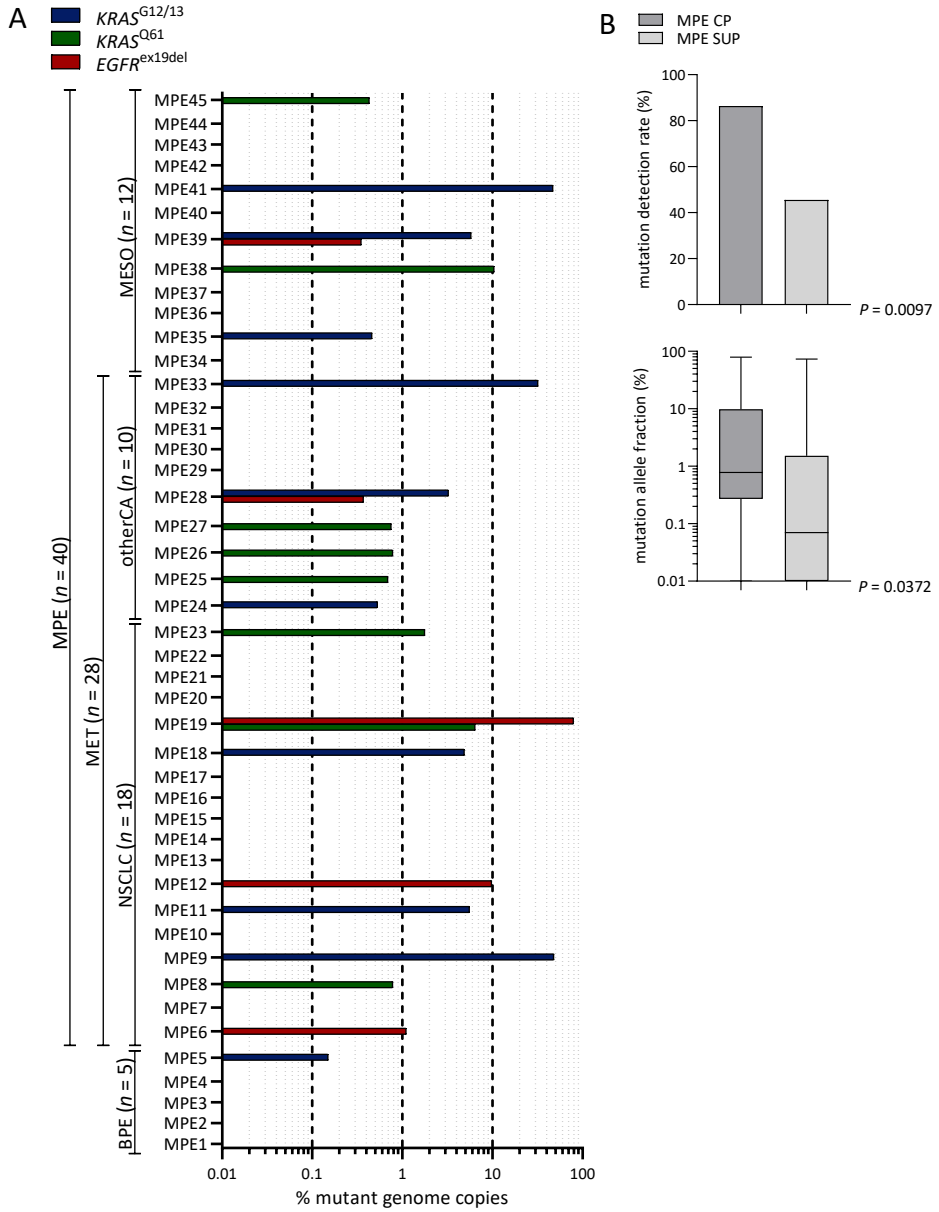

Figure 7 | Summary of the droplet digital PCR data analysis

MPE cohort's pleural effusion samples were subjected to droplet digital PCR for the detection of *KRAS* codon 12/13 (*KRAS*$^{G12/13}$) and codon 61 (*KRAS*^{Q61}) mutations, as well as *EGFR* exon 19 deletion mutations (*EGFR*^{ex19del}). (A) Shown is a data summary of the highest mutant allelic frequencies (%mut) detected per individual sample. BPE, benign pleural effusion; MESO, mesothelioma; MET, metastatic pleural malignancy, *n*, number of patients; NSCLC, non-small-cell lung carcinoma; otherCA, other metastatic cancer. (B) MPE cell pellet (CP) is superior to MPE supernatant (SUP) for rare mutation detection. Comparison of mutation detection rate and mutation allele fraction. *P*, probability, Mann-Whitney test.

Table 5 | *KRAS* and *EGFR* mutation status of the MPE cohort

Diagnosis		*n*	***KRAS*^{MUT}**	*KRAS*$^{G12/13}$	*KRAS*^{Q61}	***EGFR*^{MUT}**	Oncogene^{MUT}
MET		28	12 (42.85)	6 (21.42)	6 (21.42)	4 (14.28)	16 (57.14)
	NSCLC	18	6 (33.33)	3 (16.67)	3 (16.67)	3 (16.67)	9 (50.00)
	otherCA	10	6 (60.00)	3 (30.00)	3 (30.00)	1 (10.00)	7 (70.00)
MESO		12	5 (41.67)	3 (25.00)	2 (16.67)	1 (8.33)	6 (50.00)
total		40	**17 (42.50)**	9 (22.50)	8 (20.00)	**5 (12.50)**	22 (55.00)

Data are presented as *n* (% mutant). *n*, number of MPE samples.

MESO, mesothelioma; MET, metastatic pleural malignancy; ^{MUT}, mutant; NSCLC, non-small-cell lung carcinoma; otherCA, other metastatic cancer.

6 Discussion

6.1 The Mesothelioma Score

Malignant pleural mesothelioma represents one of the deadliest malignancies. Its incidence has risen in the last decades due to the asbestos-exposure in industrial countries in the mid to late 20th century (61). According to a WHO prediction, developing countries where the asbestos-consumption remains unregulated, might face an exponential increase of asbestos-related diseases (62). In the absence of any curative treatment option, the median survival time for mesothelioma ranges from eight to 14 months from diagnosis (63). Patients with a resectable tumor stage are offered surgical procedures, such as extrapleural pneumonectomy or extended pleurectomy/decortication, aiming for maximal macroscopic cytoreduction. The benefit of surgery is controversial but various studies assume a prognostic benefit. Due to the high operative morbidity and mortality, surgery is limited to patients with early-stage disease and a good performance status (64). Mesothelioma staging still is a major challenge that must be improved to guarantee the application of the best treatment options at the earliest timepoint of the disease. In 90% of cases mesothelioma comes with unilateral MPE at presentation and in contrast to most patients with a metastatic pleural cancer, the presence of MPE does not preclude surgery. Quite the contrary, MPE is present only at an early disease stage and tends to resolve with disease progression (63). Thus, patients with a previous asbestos exposure and MPE should be carefully monitored. The critical issue here is the low cytologic yield of MPE for mesothelioma. The disease might be missed in the first place and become apparent again at an advanced stage with limited therapeutic options left. Indeed,

patients with cytological-negative MPE show significantly shorter survival times (65). This is exactly where the Mesothelioma Score takes its stand. It can be used as an introductory screening tool for patients presenting with MPE of unknown origin, especially with a history of asbestos-exposure. By using routinely determined blood test and lung function parameters, it is possible to distinguish whether MPE originates of a primary or metastatic pleural malignancy. The Mesothelioma Score is a convenient and widely applicable diagnostic tool based on the three simple, but reliable parameters airway resistance (R), arterial partial pressure of oxygen at ambient air (paO_2) and hemoglobin (Hb). It ensures an outstanding diagnostic yield for mesothelioma, with a sensitivity of 81.82% and a specificity of 95.24%. The score raises hope for a more frequent detection of mesothelioma at an early stage of the disease, thus keeping all available treatment options open and eventually extending survival time.

A major limitation of the Mesothelioma Score is the MPE cohort´s composition. Mesothelioma patients constitute 30% of the cohort and moreover, due to missing data, contribute to the final score in a ratio of 2:1 (MET:MESO). By contrast, reviews of cytopathologic diagnoses of MPE samples yield only a marginal percentage of mesothelioma, ranging from 1-10% (7,66,67). This surplus of mesothelioma patients in the MPE cohort might distort the diagnostic yield of a score created to detect an utterly rare disease. Here arises the need of a validation cohort that reflects the regional prevalence of mesothelioma.

6.2 Prospects of targeted MPE treatment

MPE samples (*n* = 40) of patients with primary (*n* = 12) or metastatic (*n* = 28) pleural malignancies were divided by their CP and SUP, and respectively subjected to ddPCR multiplex assays for *KRAS* G12/13, *KRAS* Q61 and *EGFR* ex19del mutations. 55% of MPE samples were identified as oncogene mutant. *EGFR* and *KRAS* are both considered novel targets for MPE treatment. EGFR-TKIs are already approved as the first-line therapy for stage IV NSCLC, but further seem to affect metastatic sites (52). *EGFR* ex19del mutations were detected for 16.67% of MPE cohort's NSCLC patients. Applying EGFR-TKIs in these cases should not only be the cancer therapy of choice, but as of now should be exceedingly investigated for effects on MPE resolution. Unfortunately, tumors are most likely to develop TKI-resistance after a short period of regression (7). Hence, impeding mutant *KRAS* signaling could become a major

approach in MPE management. Agaloti et al. recently disclosed mutant *KRAS* crucial for MPE formation and novel therapeutics based on these finding are on the rise (18). However, the proposed KRAS-MPE link misses confirmation by human studies. For the MPE cohort, 42.50% of patients were assigned a *KRAS* mutation, either in codon 12/13 (22.50%) or codon 61 (20.00%). Thus, the cohort yielded a considerable higher *KRAS* mutation frequency than present studies. This confirms the hypothesis, that the fraction of *KRAS*-mutant MPE so far might have been underestimated. One possible explanation for the discrepancy could be the applied mutation detection method. Working with liquid biopsies requires an extremely sensitive technique to facilitate precise detection despised a low fractional abundance of mutant genome copies (39). Whereas Sanger sequencing and next generation sequencing are commonly applied, their LOD is inferior to the employed ddPCR technique that enables detection down to 1:20000 mutant copies (68). 40.91% of the oncogene positive MPEs displayed mutant copy numbers <1:100 and 18,18% even below 1:200. These samples could have likely been missed by other techniques. A substantial proportion of *KRAS* mutations was found in codon 61, a spot rarely sequenced though capable of MPE induction (18). Smits et all. already claimed *KRAS* Q61 mutations unseen opposed to the hotspots, codon 12 and 13 (52). Further, a surprising 41.67% of mesothelioma patients were screened *KRAS* mutant. This reconciles with the recently discovered pathogenic key role of *RAS/TP53* pathway mutations for mesothelioma and concomitant MPE (69).

To conclude, this project wants to raise attention on the diagnostic potential of pleural effusion-based liquid biopsy and the implementation of biopharmaceutics in future MPE management. Activating *EGFR* and *KRAS* mutations are believed to play a pathogenetic role in MPE induction and both are commonly detected in MPE. Especially, *KRAS* mutation frequency seems to be underestimated by present human studies, most likely due to the inadequate LOD of direct sequencing. Both oncogenes are addressable by novel biologicals that have already proven their potential in halting MPE formation in mouse models. Prospectively genotyped and longitudinally observed MPE cohorts are likely to further confirm MPE genotype–phenotype linkages and the therapeutic efficacy of EGFR-TKI and deltarasin on human MPE.

Bibliography

1. Dixit R, Agarwal KC, Gokhroo A, Patil CB, Meena M, Shah NS, et al. Diagnosis and management options in malignant pleural effusions. Lung India. 2017 Apr;34(2):160–6.

2. Bibby AC, Dorn P, Psallidas I, Porcel JM, Janssen J, Froudarakis M, et al. ERS/EACTS statement on the management of malignant pleural effusions. Eur Respir J. 2018 Jul;52(1).

3. Penz E, Watt KN, Hergott CA, Rahman NM, Psallidas I. Management of malignant pleural effusion: challenges and solutions. Cancer Manag Res. 2017;9:229–41.

4. Psallidas I, Kalomenidis I, Porcel JM, Robinson BW, Stathopoulos GT. Malignant pleural effusion: from bench to bedside. Eur Respir Rev. 2016 Jun;25(140):189–98.

5. Antony VB, Loddenkemper R, Astoul P, Boutin C, Goldstraw P, Hott J, et al. Management of malignant pleural effusions. Eur Respir J. 2001 Aug;18(2):402–19.

6. Clive AO, Kahan BC, Hooper CE, Bhatnagar R, Morley AJ, Zahan-Evans N, et al. Predicting survival in malignant pleural effusion: development and validation of the LENT prognostic score. Thorax. 2014 Dec;69(12):1098–104.

7. Skok K, Hladnik G, Grm A, Crnjac A. Malignant Pleural Effusion and Its Current Management: A Review. Medicina (Kaunas). 2019 Aug 15;55(8).

8. Hooper C, Lee YCG, Maskell N, BTS Pleural Guideline Group. Investigation of a unilateral pleural effusion in adults: British Thoracic Society Pleural Disease Guideline 2010. Thorax. 2010 Aug;65 Suppl 2:ii4-17.

9. Loveland P, Christie M, Hammerschlag G, Irving L, Steinfort D. Diagnostic yield of pleural fluid cytology in malignant effusions: an Australian tertiary centre experience. Intern Med J. 2018 Nov;48(11):1318–24.

10. Menzies R, Charbonneau M. Thoracoscopy for the diagnosis of pleural disease. Ann Intern Med. 1991 Feb 15;114(4):271–6.

11. Eccher A, Girolami I, Lucenteforte E, Troncone G, Scarpa A, Pantanowitz L. Diagnostic mesothelioma biomarkers in effusion cytology. Cancer Cytopathol. 2021 Jul;129(7):506–16.

12. Brown RW, Clark GM, Tandon AK, Allred DC. Multiple-marker immunohistochemical phenotypes distinguishing malignant pleural mesothelioma from pulmonary adenocarcinoma. Hum Pathol. 1993 Apr;24(4):347–54.

13. Domínguez-Malagón H, Cano-Valdez AM, González-Carrillo C, Campos-Salgado YE, Lara-Garcia A, Lopez-Mejia M, et al. Diagnostic efficacy of electron microscopy and pleural effusion cytology for the distinction of pleural mesothelioma and lung adenocarcinoma. Ultrastruct Pathol. 2016 Oct;40(5):254–60.

14. Martínez-Moragón E, Aparicio J, Sanchis J, Menéndez R, Cruz Rogado M, Sanchis F. Malignant pleural effusion: prognostic factors for survival and response to chemical pleurodesis in a series of 120 cases. Respiration. 1998;65(2):108–13.

15. Koegelenberg CFN, Shaw JA, Irusen EM, Lee YCG. Contemporary best practice in the management of malignant pleural effusion. Ther Adv Respir Dis. 2018 Dec;12:1753466618785098.

16. Iyer NP, Reddy CB, Wahidi MM, Lewis SZ, Diekemper RL, Feller-Kopman D, et al. Indwelling Pleural Catheter versus Pleurodesis for Malignant Pleural Effusions. A Systematic Review and Meta-Analysis. Ann Am Thorac Soc. 2019 Jan;16(1):124–31.

17. Rial MB, Lamela IP, Fernández VL, Arca JA, Delgado MN, Pombo CV, et al. Management of malignant pleural effusion by an indwelling pleural catheter: A cost-efficiency analysis. Ann Thorac Med. 2015 Sep;10(3):181–4.

18. Agalioti T, Giannou AD, Krontira AC, Kanellakis NI, Kati D, Vreka M, et al. Mutant KRAS promotes malignant pleural effusion formation. Nat Commun. 2017 16;8:15205.

19. Stathopoulos GT, Kalomenidis I. Malignant pleural effusion: tumor-host interactions unleashed. Am J Respir Crit Care Med. 2012 Sep 15;186(6):487–92.

20. Marazioti A, Lilis I, Vreka M, Apostolopoulou H, Kalogeropoulou A, Giopanou I, et al. Myeloid-derived interleukin-1β drives oncogenic KRAS-NF-κB addiction in malignant pleural effusion. Nat Commun. 2018 Feb 14;9(1):672.

21. Agalioti T, Giannou AD, Stathopoulos GT. Pleural involvement in lung cancer. J Thorac Dis. 2015 Jun;7(6):1021–30.

22. Marazioti A, Kairi CA, Spella M, Giannou AD, Magkouta S, Giopanou I, et al. Beneficial impact of CCL2 and CCL12 neutralization on experimental malignant pleural effusion. PLoS One. 2013;8(8):e71207.

23. Esagian SM, Grigoriadou GI, Nikas IP, Boikou V, Sadow PM, Won J-K, et al. Comparison of liquid-based to tissue-based biopsy analysis by targeted next generation sequencing in advanced non-small cell lung cancer: a comprehensive systematic review. J Cancer Res Clin Oncol. 2020 Aug;146(8):2051–66.

24. Russano M, Napolitano A, Ribelli G, Iuliani M, Simonetti S, Citarella F, et al. Liquid biopsy and tumor heterogeneity in metastatic solid tumors: the potentiality of blood samples. Journal of Experimental & Clinical Cancer Research. 2020 May 27;39(1):95.

25. Gerlinger M, Rowan AJ, Horswell S, Larkin J, Endesfelder D, Gronroos E, et al. Intratumor Heterogeneity and Branched Evolution Revealed by Multiregion Sequencing. New England Journal of Medicine. 2012 Mar 8;366(10):883–92.

26. Spella M, Giannou AD, Stathopoulos GT. Switching off malignant pleural effusion formation-fantasy or future? J Thorac Dis. 2015 Jun;7(6):1009–20.

27. Ilié M, Hofman P. Pros: Can tissue biopsy be replaced by liquid biopsy? Transl Lung Cancer Res. 2016 Aug;5(4):420–3.

28. Heitzer E, Haque IS, Roberts CES, Speicher MR. Current and future perspectives of liquid biopsies in genomics-driven oncology. Nat Rev Genet. 2019 Feb;20(2):71–88.

29. Poulet G, Massias J, Taly V. Liquid Biopsy: General Concepts. Acta Cytol. 2019;63(6):449–55.

30. Ou S-HI, Nagasaka M, Zhu VW. Liquid Biopsy to Identify Actionable Genomic Alterations. Am Soc Clin Oncol Educ Book. 2018 May 23;38:978–97.

31. Alix-Panabières C, Pantel K. Clinical Applications of Circulating Tumor Cells and Circulating Tumor DNA as Liquid Biopsy. Cancer Discov. 2016 May;6(5):479–91.

32. Siravegna G, Marsoni S, Siena S, Bardelli A. Integrating liquid biopsies into the management of cancer. Nat Rev Clin Oncol. 2017 Sep;14(9):531–48.

33. Guo Z, Xie Z, Shi H, Du W, Peng L, Han W, et al. Malignant pleural effusion supernatant is an alternative liquid biopsy specimen for comprehensive mutational profiling. Thorac Cancer. 2019 Apr;10(4):823–31.

34. Song Z, Wang W, Li M, Liu J, Zhang Y. Cytological-negative pleural effusion can be an alternative liquid biopsy media for detection of EGFR mutation in NSCLC patients. Lung Cancer. 2019 Oct;136:23–9.

35. Kang JY, Park CK, Yeo CD, Lee HY, Rhee CK, Kim SJ, et al. Comparison of PNA clamping and direct sequencing for detecting KRAS mutations in matched tumour tissue, cell block, pleural effusion and serum from patients with malignant pleural effusion. Respirology. 2015 Jan;20(1):138–46.

36. Baburaj G, Damerla RR, Udupa KS, Parida P, Munisamy M, Kolesar J, et al. Liquid biopsy approaches for pleural effusion in lung cancer patients. Mol Biol Rep. 2020 Oct;47(10):8179–87.

37. Yang J, Lee O-J, Son S-M, Woo CG, Jeong Y, Yang Y, et al. EGFR Mutation Status in Lung Adenocarcinoma-Associated Malignant Pleural Effusion and Efficacy of EGFR Tyrosine Kinase Inhibitors. Cancer Res Treat. 2018 Jul;50(3):908–16.

38. Kimura H, Fujiwara Y, Sone T, Kunitoh H, Tamura T, Kasahara K, et al. EGFR mutation status in tumour-derived DNA from pleural effusion fluid is a practical basis for predicting the response to gefitinib. Br J Cancer. 2006 Nov 20;95(10):1390–5.

39. Elazezy M, Joosse SA. Techniques of using circulating tumor DNA as a liquid biopsy component in cancer management. Computational and Structural Biotechnology Journal. 2018 Jan 1;16:370–8.

40. Isler JA, Vesterqvist OE, Burczynski ME. Analytical validation of genotyping assays in the biomarker laboratory. Pharmacogenomics. 2007 Apr;8(4):353–68.

41. Lin M-T, Mosier SL, Thiess M, Beierl KF, Debeljak M, Tseng L-H, et al. Clinical validation of KRAS, BRAF, and EGFR mutation detection using next-generation sequencing. Am J Clin Pathol. 2014 Jun;141(6):856–66.

42. Zonta E, Garlan F, Pécuchet N, Perez-Toralla K, Caen O, Milbury C, et al. Multiplex Detection of Rare Mutations by Picoliter Droplet Based Digital PCR: Sensitivity and Specificity Considerations. PLOS ONE. 2016 Jul 14;11(7):e0159094.

43. Liu J-Y, Xiong L, Zhang M, Shuai S-Y, Wei X-S, Ye L-L, et al. Medical thoracoscopy in China-the present status and the future. J Thorac Dis. 2017 Feb;9(2):406–13.

44. Agrawal A, Tandon R, Singh L, Chawla A. Clinico- pathological profile and course of malignant pleural effusion in a tertiary care teaching hospital in western U.P. with special reference to lung cancer. Lung India. 2015;32(4):326–30.

45. Zhang H, Li C, Hu F, Zhang X, Shen Y, Chen Y, et al. Auxiliary diagnostic value of tumor biomarkers in pleural fluid for lung cancer-associated malignant pleural effusion. Respir Res. 2020 Oct 29;21(1):284.

46. Bakhshayesh Karam M, Karimi S, Mosadegh L, Chaibakhsh S. Malignant Mesothelioma Versus Metastatic Carcinoma of the Pleura: A CT Challenge. Iran J Radiol. 2016 Jan;13(1):e10949.

47. Zhang X, Duan H, Yu Y, Ma C, Ren Z, Lei Y, et al. Differential diagnosis between benign and malignant pleural effusion with dual-energy spectral CT. PLoS One. 2018;13(4):e0193714.

48. Keedy VL, Temin S, Somerfield MR, Beasley MB, Johnson DH, McShane LM, et al. American Society of Clinical Oncology provisional clinical opinion: epidermal growth factor receptor (EGFR) Mutation testing for patients with advanced non-small-cell lung cancer considering first-line EGFR tyrosine kinase inhibitor therapy. J Clin Oncol. 2011 May 20;29(15):2121–7.

49. Sharma SV, Bell DW, Settleman J, Haber DA. Epidermal growth factor receptor mutations in lung cancer. Nat Rev Cancer. 2007 Mar;7(3):169–81.

50. Lin J-B, Lai F-C, Li X, Tu Y-R, Lin M, Qiu M-L, et al. Sequential treatment strategy for malignant pleural effusion in non-small cell lung cancer with the activated epithelial grow factor receptor mutation. J Drug Target. 2017 Feb;25(2):119–24.

51. Shamblin CJ, Tanner NT, Sanchez RS, Woolworth JA, Silvestri GA. EGFR mutations in malignant pleural effusions from lung cancer. Curr Respir Care Rep. 2013 Jun 1;2(2):79–87.

52. Smits AJJ, Kummer JA, Hinrichs JWJ, Herder GJM, Scheidel-Jacobse KC, Jiwa NM, et al. EGFR and KRAS mutations in lung carcinomas in the Dutch population: increased EGFR mutation frequency in malignant pleural effusion of lung adenocarcinoma. Cell Oncol (Dordr). 2012 Jun;35(3):189–96.

53. Choi SY, Kim HW, Jeon SH, Kim BN, Kang N, Yeo CD, et al. Comparison of PANAMutyper and PNAClamp for Detecting KRAS Mutations from Patients With Malignant Pleural Effusion. In Vivo. 2019 Jun;33(3):945–54.

54. DeMaio A, Clarke JM, Dash R, Sebastian S, Wahidi MM, Shofer SL, et al. Yield of Malignant Pleural Effusion for Detection of Oncogenic Driver Mutations in Lung Adenocarcinoma. J Bronchology Interv Pulmonol. 2019 Apr;26(2):96–101.

55. Cancer Genome Atlas Research Network. Comprehensive molecular profiling of lung adenocarcinoma. Nature. 2014 Jul 31;511(7511):543–50.

56. Lee T, Lee B, Choi Y-L, Han J, Ahn M-J, Um S-W. Non-small Cell Lung Cancer with Concomitant EGFR, KRAS, and ALK Mutation: Clinicopathologic Features of 12 Cases. J Pathol Transl Med. 2016 May;50(3):197–203.

57. Klotz LV, Courty Y, Lindner M, Petit-Courty A, Stowasser A, Koch I, et al. Comprehensive clinical profiling of the Gauting locoregional lung adenocarcinoma donors. Cancer Med. 2019 Apr;8(4):1486–99.

58. Ponce MC, Sharma S. Pulmonary Function Tests. In: StatPearls [Internet]. Treasure Island (FL): StatPearls Publishing; 2021 [cited 2021 May 16]. Available from: http://www.ncbi.nlm.nih.gov/books/NBK482339/

59. Campbell EJM. Respiratory Failure. Br Med J. 1965 Jun 5;1(5448):1451–60.

60. Herbinger K-H, Hanus I, Beissner M, Berens-Riha N, Kroidl I, von Sonnenburg F, et al. Lymphocytosis and Lymphopenia Induced by Imported Infectious Diseases: A Controlled Cross-Sectional Study of 17,229 Diseased German Travelers Returning from the Tropics and Subtropics. Am J Trop Med Hyg. 2016 Jun 1;94(6):1385–91.

61. Subotic D. Malignant pleural effusion and mesothelioma. AME Medical Journal; Vol 5 (March 2020): AME Medical Journal [Internet]. 2020 [cited 2020 Jan 1]; Available from: https://amj.amegroups.com/article/view/5427

62. Kameda T, Takahashi K, Kim R, Jiang Y, Movahed M, Park E-K, et al. Asbestos: use, bans and disease burden in Europe. Bull World Health Organ. 2014 Nov 1;92(11):790–7.

63. Bibby AC, Tsim S, Kanellakis N, Ball H, Talbot DC, Blyth KG, et al. Malignant pleural mesothelioma: an update on investigation, diagnosis and treatment. Eur Respir Rev. 2016 Dec;25(142):472–86.

64. Cantini L, Hassan R, Sterman DH, Aerts JGJV. Emerging Treatments for Malignant Pleural Mesothelioma: Where Are We Heading? Front Oncol. 2020;10:343.

65. Negi Y, Kuribayashi K, Funaguchi N, Doi H, Mikami K, Minami T, et al. Early-stage Clinical Characterization of Malignant Pleural Mesothelioma. In Vivo. 2018 Oct;32(5):1169–74.

66. Johnston WW. The malignant pleural effusion. A review of cytopathologic diagnoses of 584 specimens from 472 consecutive patients. Cancer. 1985 Aug 15;56(4):905–9.

67. Koegelenberg CFN, Bennji SM, Boer E, Schubert PT, Shaw JA, Allwood BW, et al. The current aetiology of malignant pleural effusion in the Western Cape Province, South Africa. S Afr Med J. 2018 Mar 28;108(4):275–7.

68. Dong L, Wang S, Fu B, Wang J. Evaluation of droplet digital PCR and next generation sequencing for characterizing DNA reference material for KRAS mutation detection. Sci Rep. 2018 Nov 30;8(1):9650.

69. Marazioti A, Krontira AC, Behrend SJ, Giotopoulou GA, Ntaliarda G, Blanquart C, et al. KRAS signaling in malignant pleural mesothelioma. EMBO Mol Med. 2021 Dec 13;e13631.

Acknowledgement

I am very grateful for all the experiences and learnings that came along with this thesis. My supervisors Prof. Dr. Stathopoulos and Prof. Dr. Behr supported me unconditionally from day one and helped me become not only a better clinician but a scientist. Prof. Stathopoulos hired me trustingly after just one skype-meeting and hence offered me the great opportunity to learn science from an amazing research team. Thank you, Georgios for all the doors you opened for me. And thanks to my wonderful colleagues: Anne-Sophie Lamort, Mario Pepe, Kristina Arendt, Sabine Behrend and Georgia Giotopoulou and the Greek research group. I started from zero, not even knowing how to handle a pipette and them all teached me science. Still, without the financial support of the GRK Research Training Group 2338, I wouldn't have been able to focus that deeply on my scientific work. Being supported by Prof. Dr. Gudermann, PD Dr. Staab-Weijnitz and Dr. Julia Brandt was a privilege. Also, I really appreciate all the support from Dr. Ina Koch and her lovely colleagues at the Asklepios Biobank. Last but not least, I want to thank Thomas, the best seat neighbor ever - thanks for all the laughter and shared candies.

Affidavit/Eidesstattliche Versicherung

Hackl, Caroline Maria

Ich erkläre hiermit an Eides statt,
dass ich die vorliegende Dissertation mit dem Titel

Molecular and clinical characterization of malignant pleural effusions.

selbständig verfasst, mich außer der angegebenen keiner weiteren Hilfsmittel bedient und alle Erkenntnisse, die aus dem Schrifttum ganz oder annähernd übernommen sind, als solche kenntlich gemacht und nach ihrer Herkunft unter Bezeichnung der Fundstelle einzeln nachgewiesen habe.
Ich erkläre des Weiteren, dass die hier vorgelegte Dissertation nicht in gleicher oder in ähnlicher Form bei einer anderen Stelle zur Erlangung eines akademischen Grades eingereicht wurde.

München, 12.08.2022 Caroline Maria Hackl